Opportunities and Challenges in Predicting Monsoon ISOs

B. N. Goswami

Indian Institute of Tropical Meteorology (IITM), Pune

Active-break spells (cycles)

Daily rainfall (mm/day) over central India for three years, 1972, 1986 and 1988

The smooth curve shows long term mean.

Red shows above normal or wet spells while **blue** shows below normal or dry spells

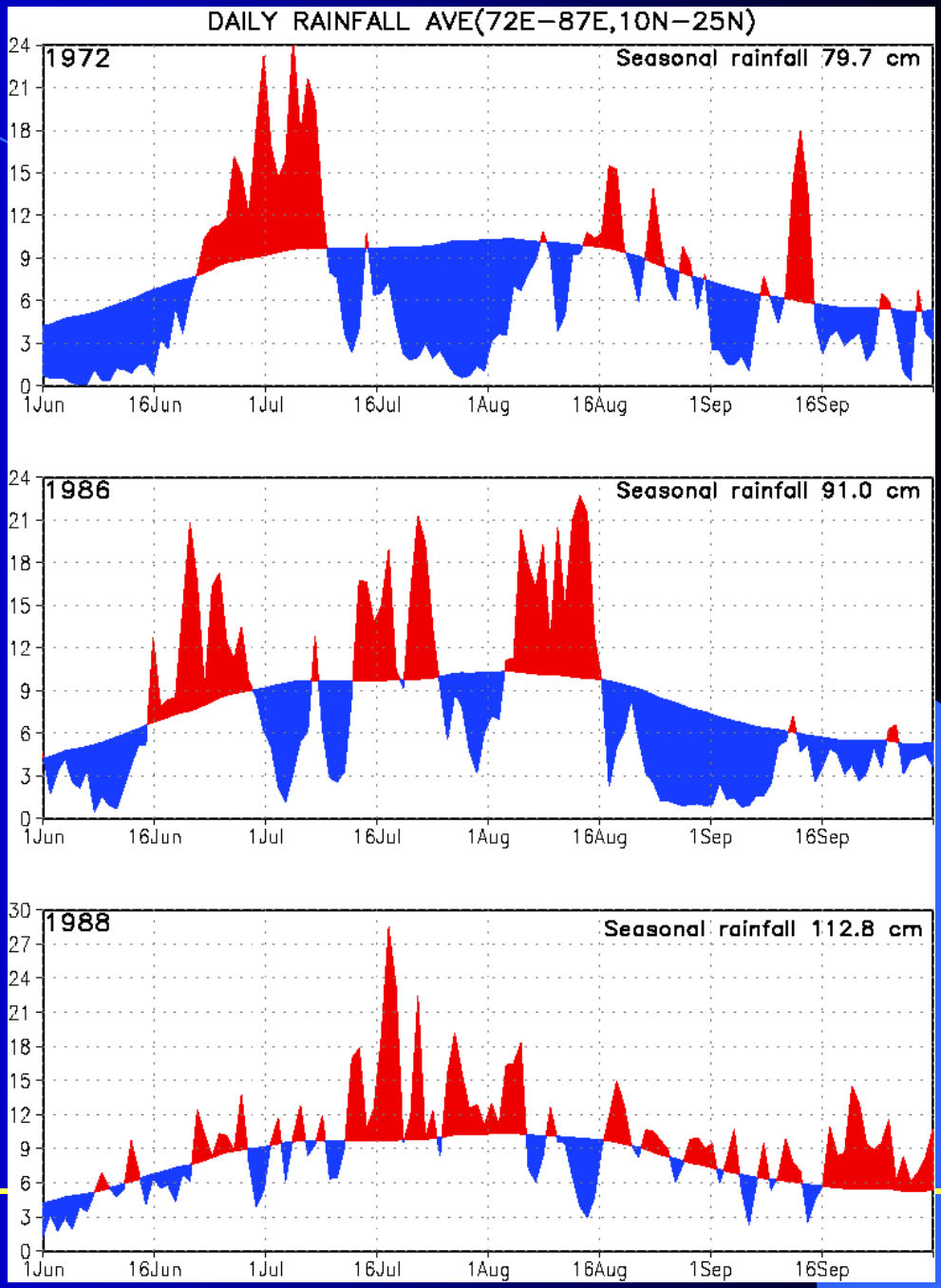

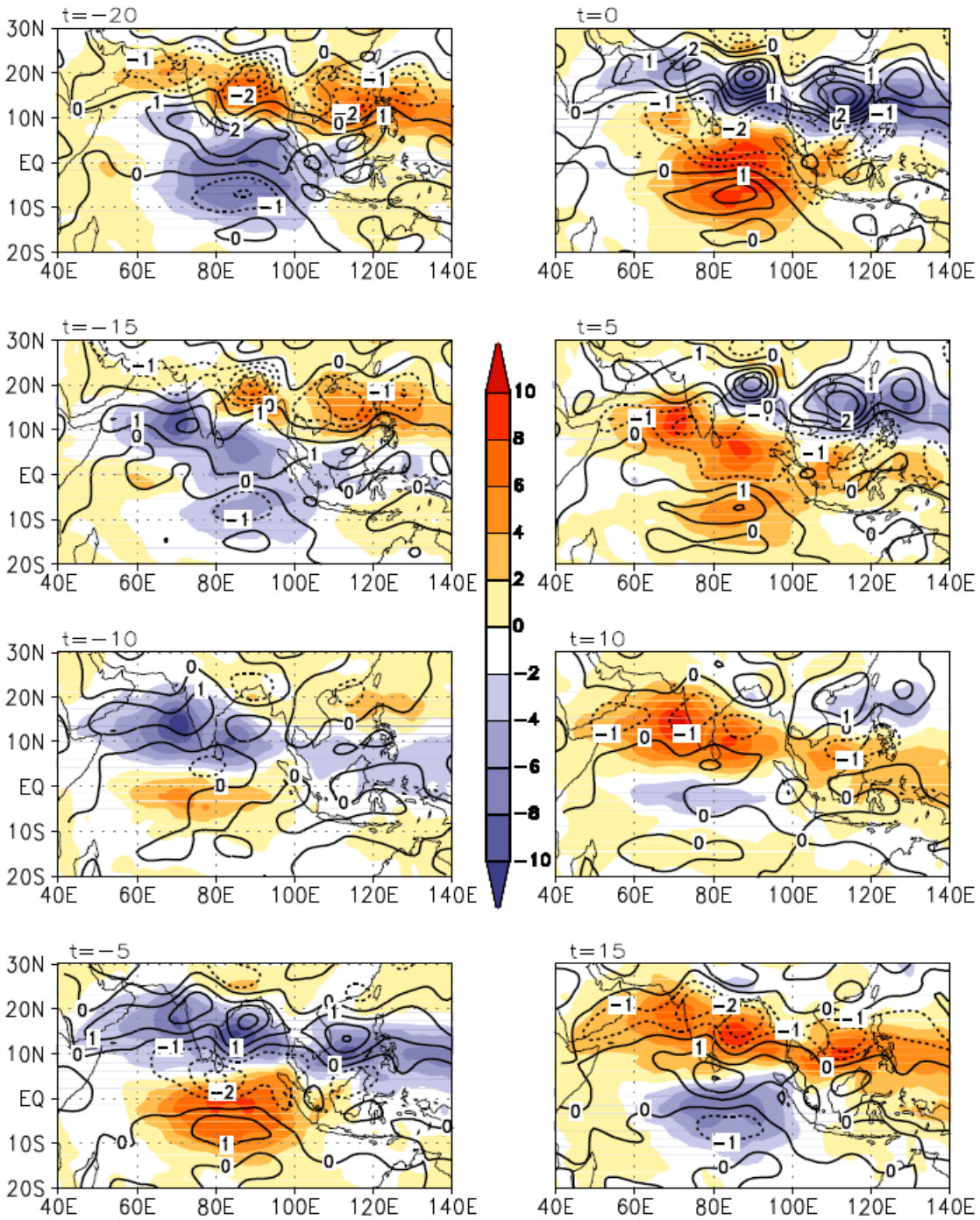

- Has a strong quasi-periodic component
- Convectively coupled with coherent northward propagation
- Nonlinear with event-to-event variability

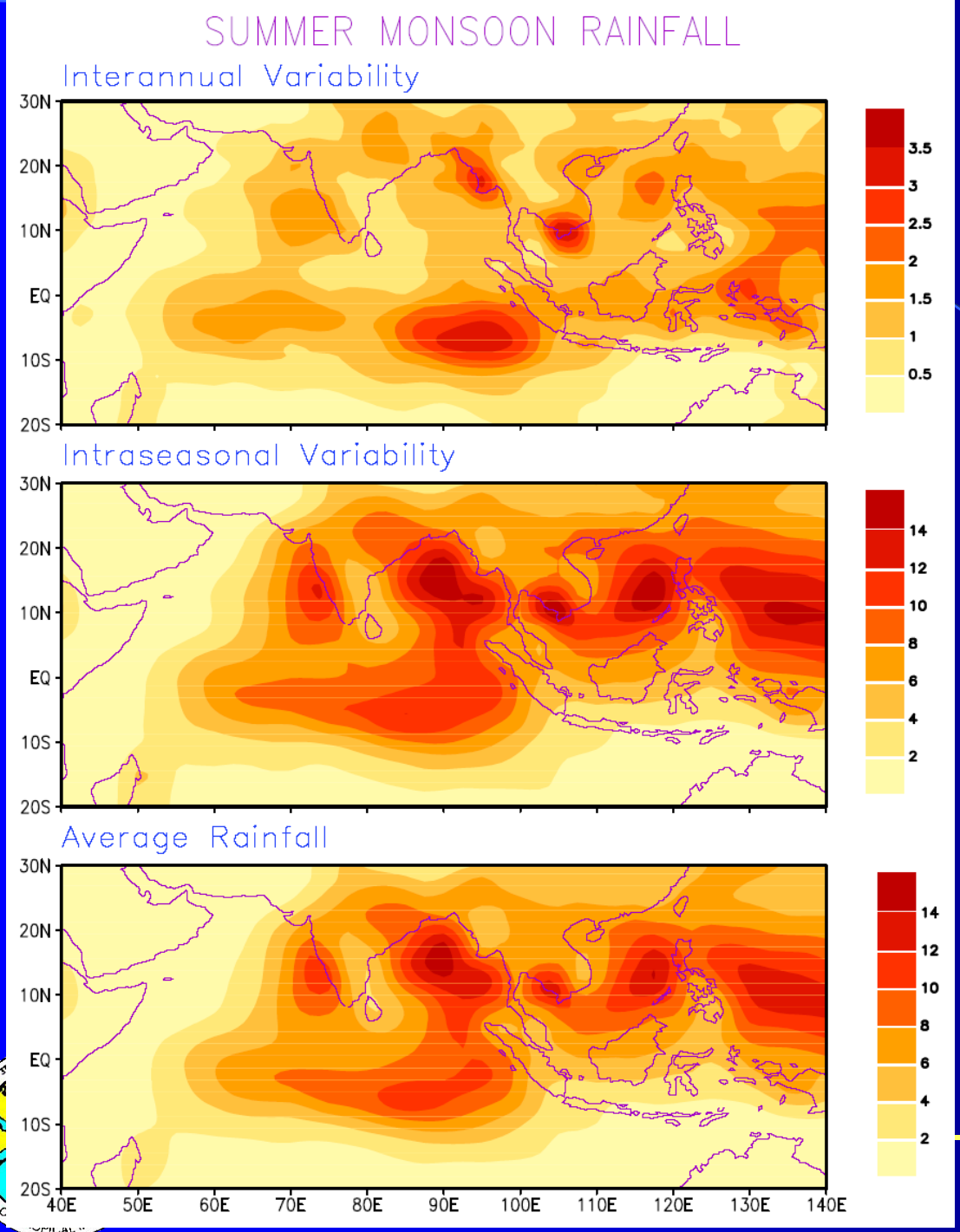

The ISO signal is much larger than signal in IAV of monsoon

Amplitude of (s.d.) of interannual variability of JJAS precipitation (mm/day) , (middle) Amplitude of intraseasonal variability (s.d. Of 10-90 day filtered anomalies during June 1 – Sept. 30) and (bottom) climatological mean JJAS precipitation (mm/day).

Potential predictability of monsoon ISOs

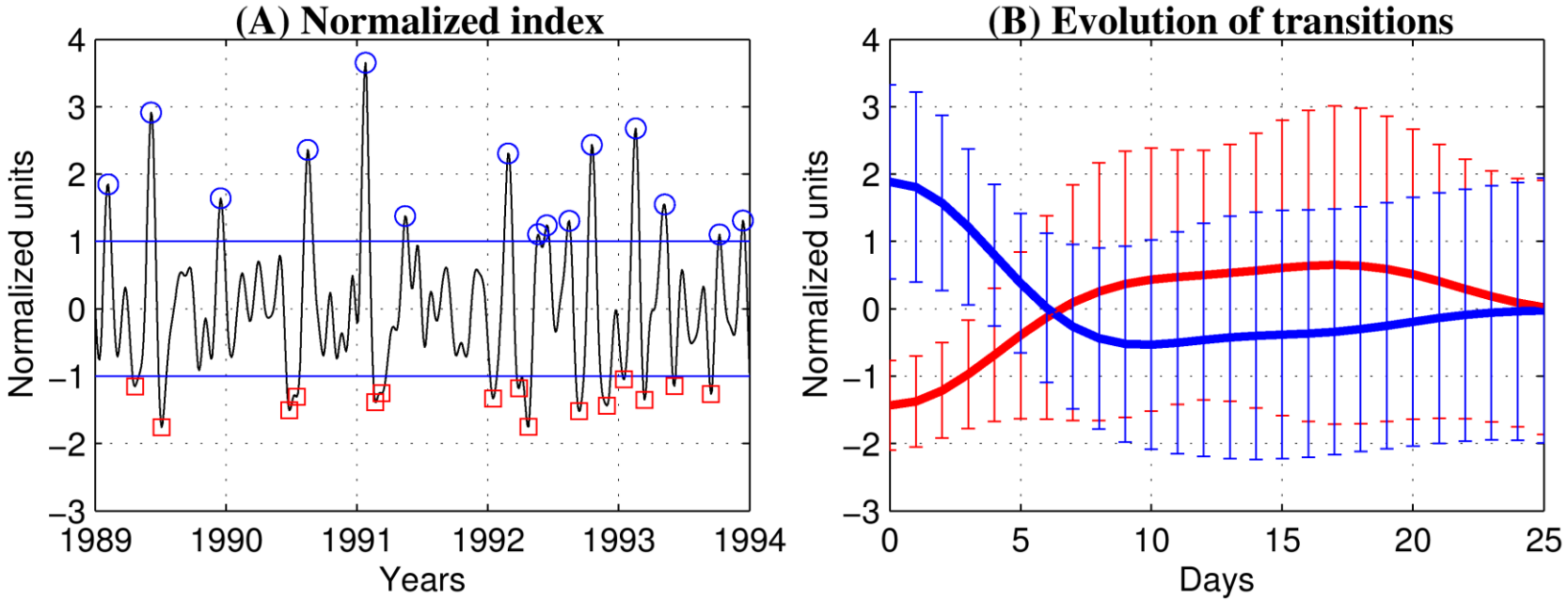

FIGURE 7.2: (A) An index of the monsoon intraseasonal variability defined as the time series of rainfall anomalies averaged over, 70°-90°E, 15°-25°N and normalised with its own standard deviation. The index is shown for a typical period of 4 years. Active phases are marked with red circles and break phases are marked with blue squares. (B) shows the evolution from active to break (in blue) and from break to active (in red). Average transitions are plotted in thick lines and the spread in transitions in terms of standard deviation of different evolutions at each lag are plotted as error bars with corresponding colours.

Goswami and Xavier, 2003, GRL, doi:10.1029/2003GL017810

For a rainfall index averaged over 70E-90E,15N-25N

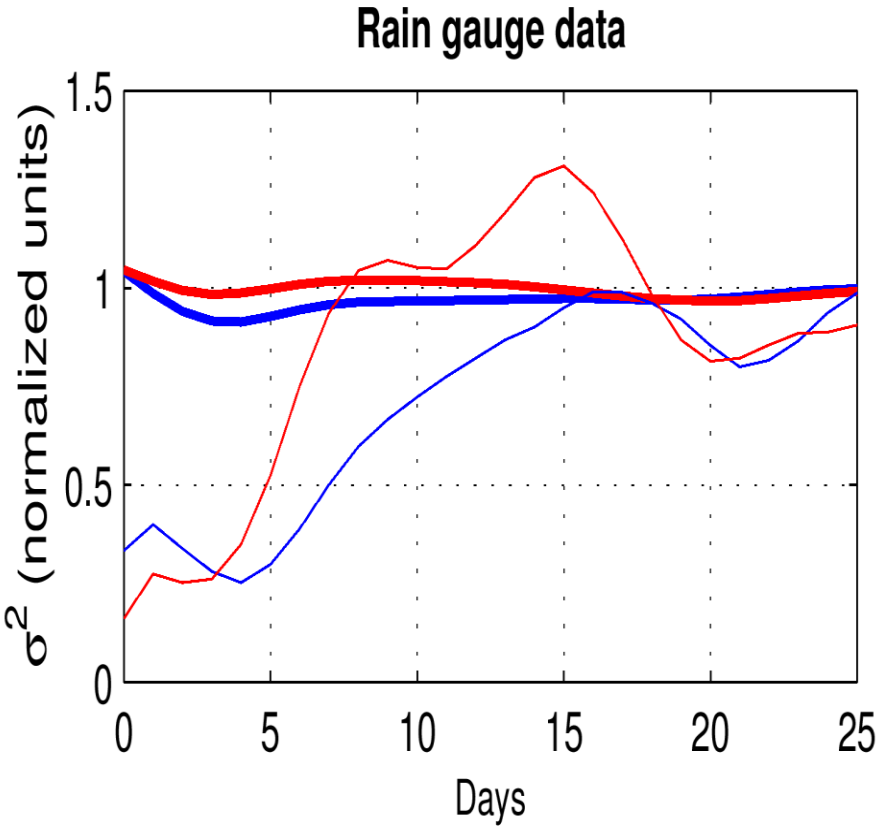

FIGURE 7.4: Same as Fig.7.3A, but for high resolution gridded daily rain gauge data (Rajeevan et al., 2006) for the JJAS season of 1951-2003.

Goswami and Xavier, 2003, GRL, doi:10.1029/2003GL017810

BACKGROUND

- **Opportunities**
  - **Potential predictability of Monsoon ISOs (MISOs) have increased in recent years compared to previous decades**
    - **Neena and Goswami. 2010, *Q. J. R. Meteorol. Soc. 136: 583–592)***
- **Challenges**
  - **New processes, not known so far, are discovered to influence event-to-event variability of observed MISO**
    - **Manoj et al. 2010 , Clim. Dyn**
    - **Neena et al., 2011, JGR**

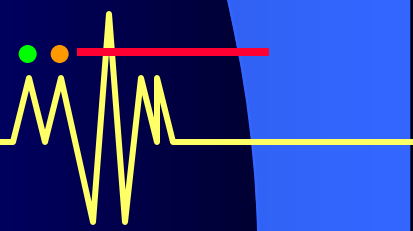

- Using IMD's 104 (1901-2004) years daily gridded rainfall data (1 × 1°) (Rajeevan et al 2008) for the June to September period, we examined the potential predictability change of active and break spells .

- In each 15 year window, a normalized ISO index is constructed by averaging the 10-90 day filtered rainfall anomalies over the monsoon trough region (70.5 E-90.5 E, 15.5 N-25.5 N) and then dividing by its own standard deviation, Goswami and Xavier (2003).

- The active and break spells were identified as when the normalized index was >= +1.0 or <= -1.0 for three or more consecutive days.

- The peak of each event was identified and signal and error estimates were made, starting from these peaks up to 30 days lead time.

Goswami and Xavier 2003, empirical method to estimate the potential predictability of active and break spells from the observed data.

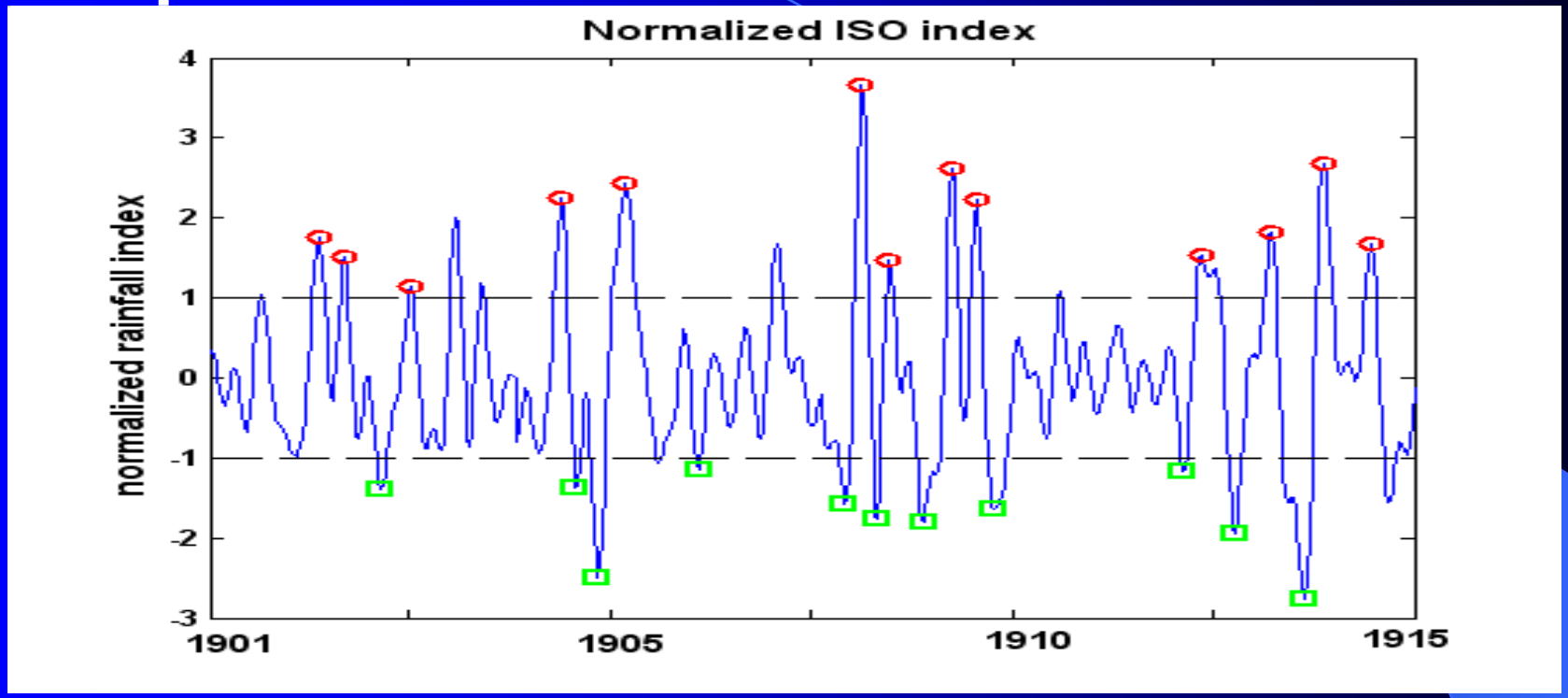

10-90 day filtered precipitation averaged over Central India normalized by its own standard deviation for 15 summers (1June-30Sep). Red Circles → Peak wet spells (active conditions); green squares → peak dry spells (break in monsoon).

- Corresponding to each lead day the signal (amplitude of the ISO) is found as the variance of 50 days starting from that particular lead day (covering approximately one complete ISO event) and averaged over all events.

- 'Error' is defined as the variance among the different active / break events corresponding to each lead day. For example, the variance between all peak active (break) days may be considered 'initial error' for the active-to-break (break-to-active) transitions. Predictability limit for evolutions starting from active / break peaks is found from the lead time when the 'error' grows and becomes as large as the signal.

- The potential predictability of any event is sensitively dependent on the error in estimating the initial condition as well as the strength of the signal.

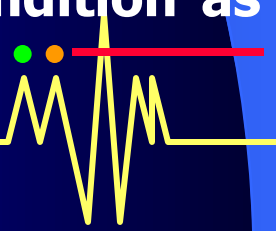

Change in potential predictability of rainfall ISO through a 15 year sliding window .

Potential predictability for evolution from active to break

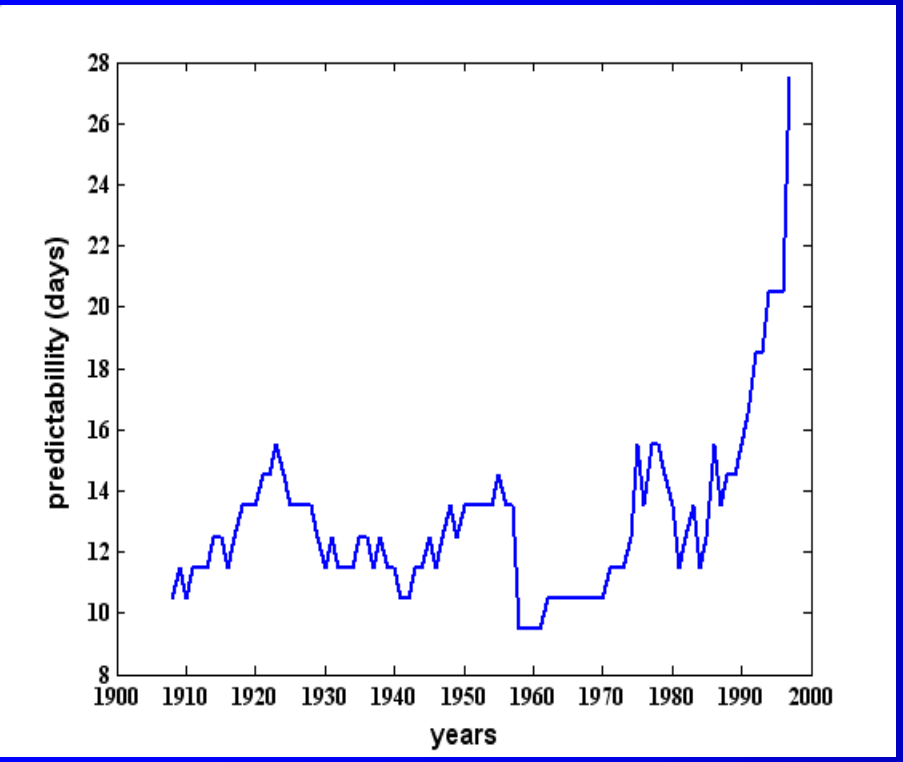

Potential predictability for evolution from break to active.

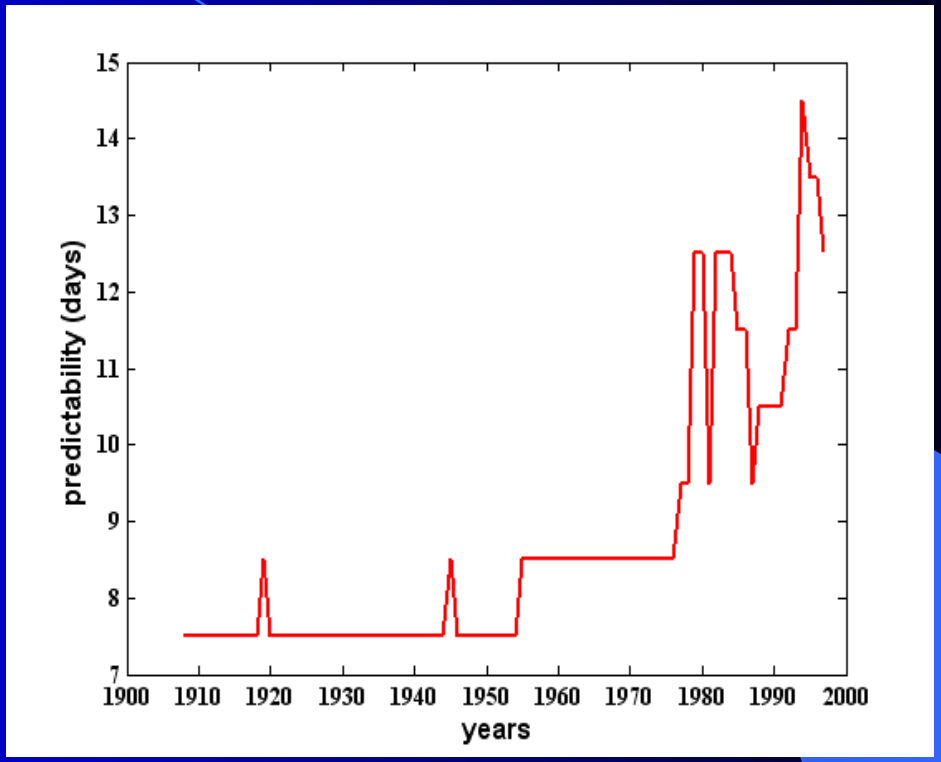

Potential predictability of breaks have increased from two weeks to three weeks and that of active increased from one week to two weeks.

Change in potential predictability of 850hPa vorticity through a 15 year sliding window .

Potential predictability for evolution from active to break

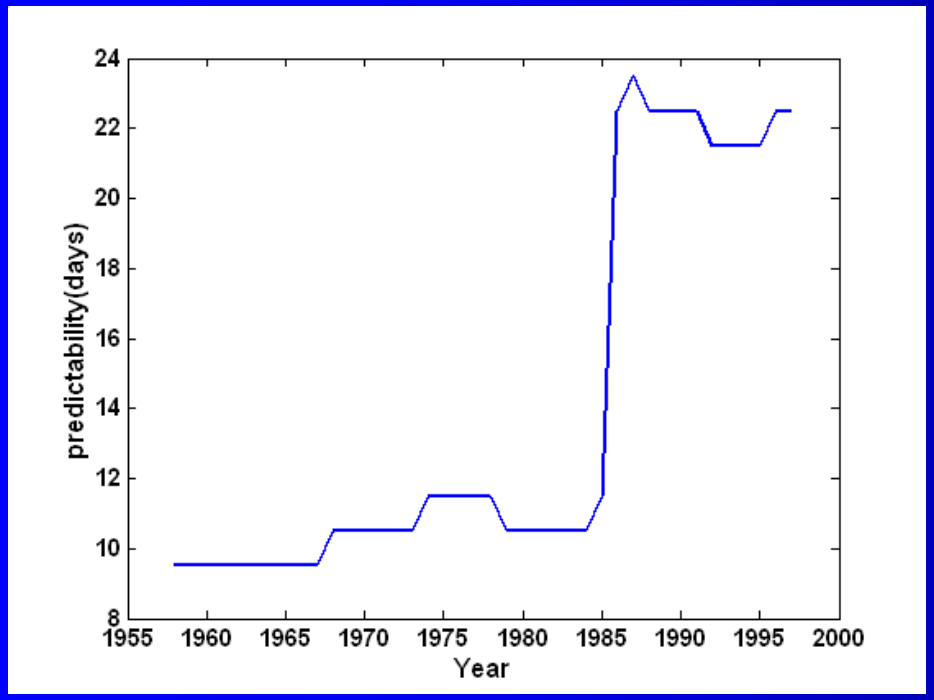

Potential predictability for evolution from break to active.

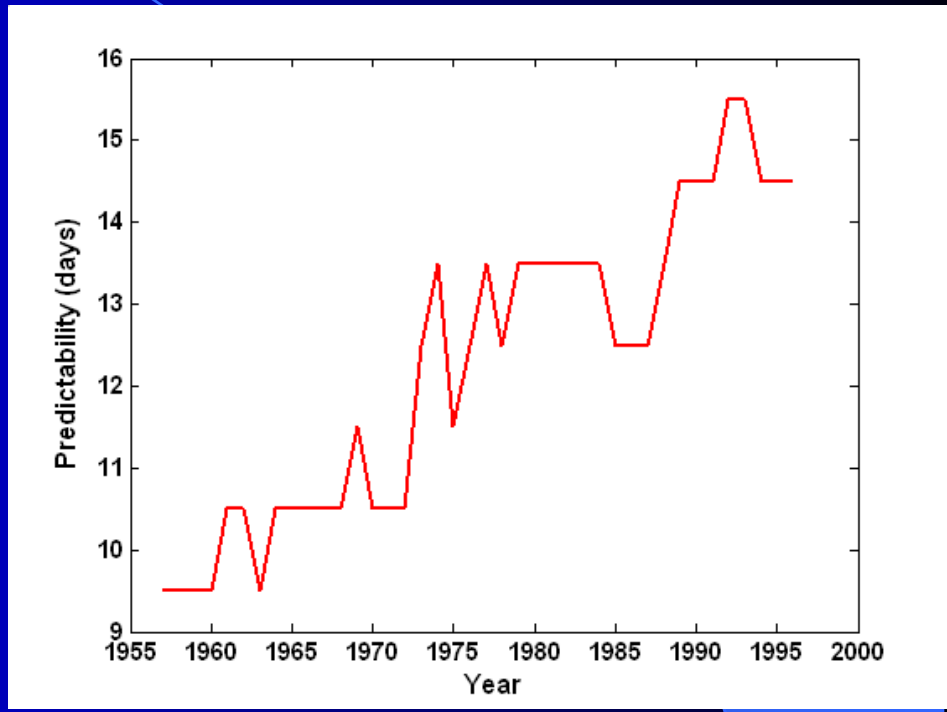

The increase in potential predictability of active/break phases in 850hPa vorticity confirms that observed in rainfall.

Changes in Initial error

active phases (red) and break phases (black).

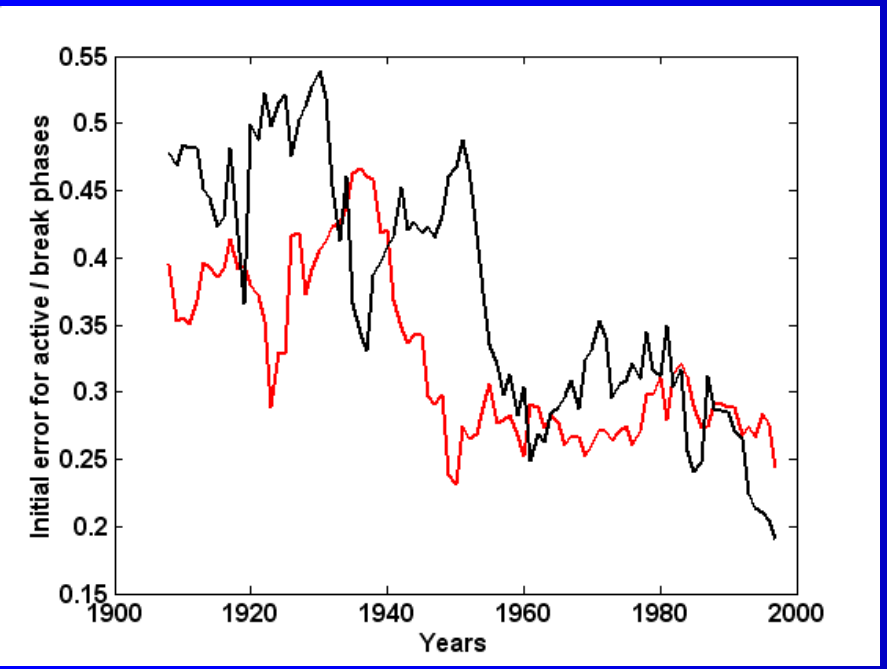

Changes in error growth characteristics

active to break (red) and break to active (black).

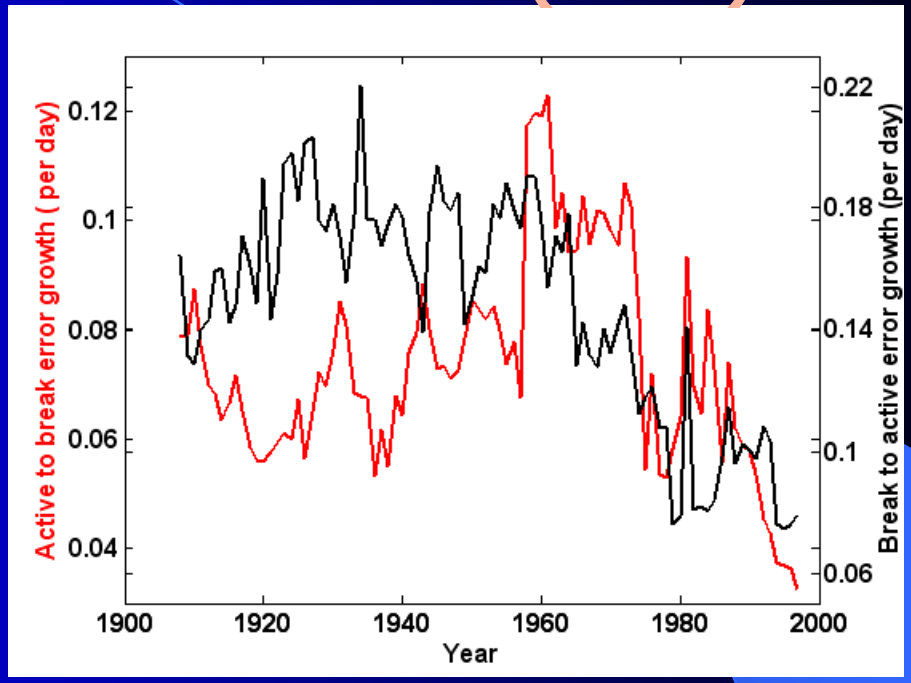

There is event to event variability in the magnitude of ISO Peaks. Thus, monsoon ISO's seems to have become increasingly more similar in recent years.

Changes in error growth is different from that of initial error, implying some other control mechanism.

KE of 30-60day mode (solid line) and 10-20 day mode (dashed line) over 60-110E, 5S-27.5N.

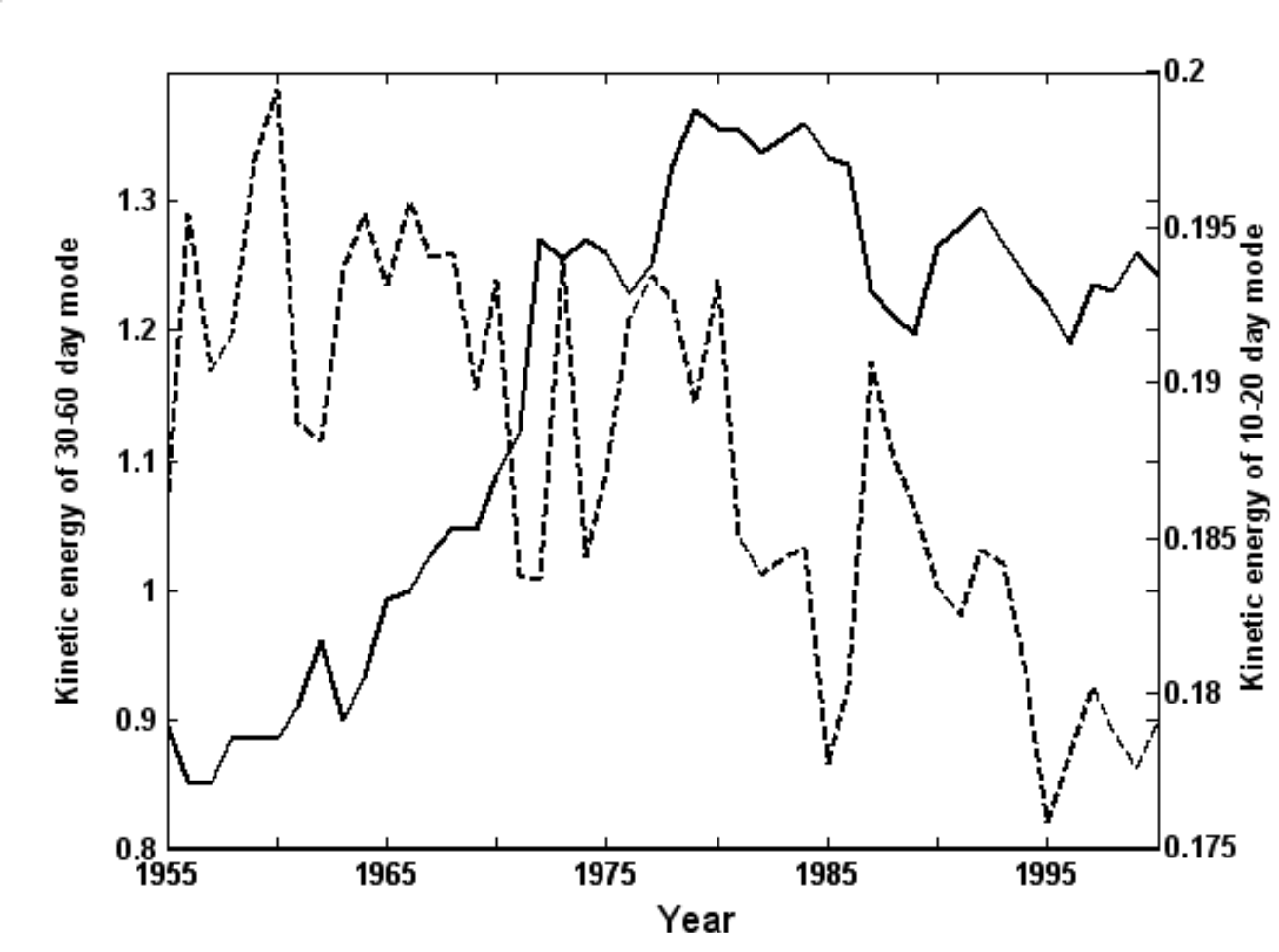

- **The changing climate seems to have decreased the predictability of the monsoon weather (Neena,Suhas and Goswami, 2009) but**

- **Increased the predictability of monsoon ISOs (active-break spells).**

- **Is the upscale cascade of errors from small scale to large scales non-uniform?**

- **To test this, we carried an extensive study of interactions between different scales using non-linear triad interactions.**

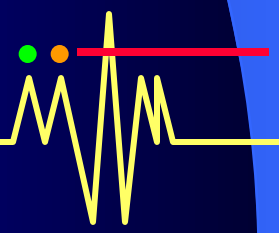

Synoptic-ISO scale interactions

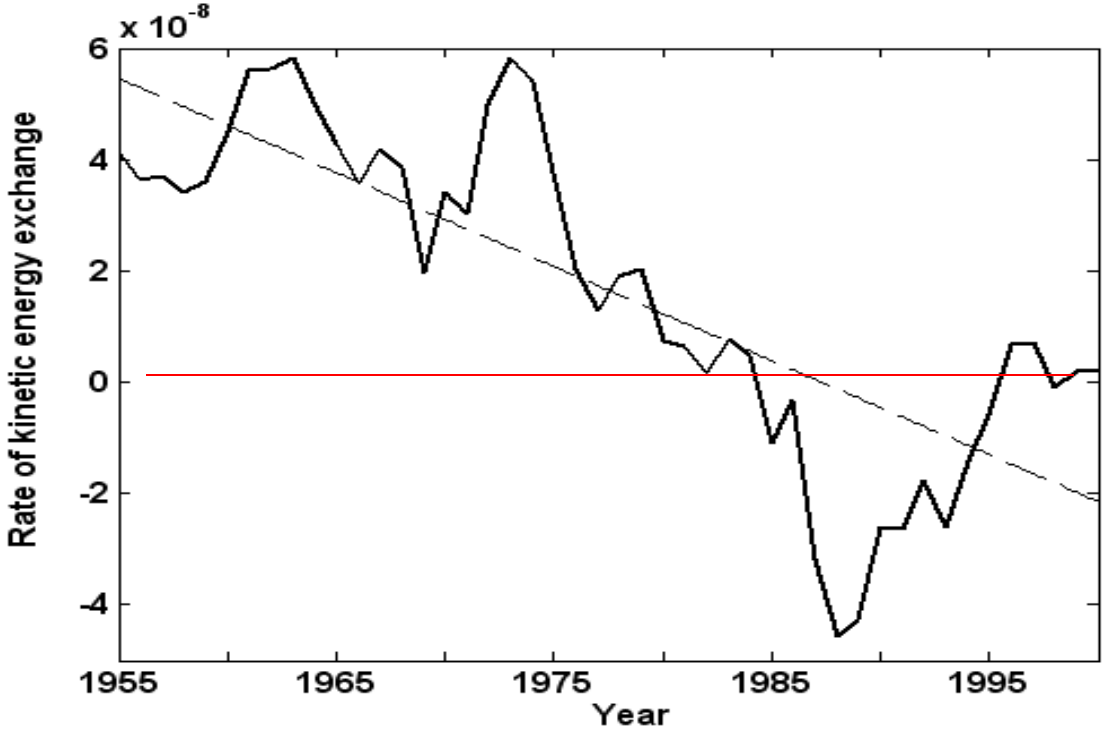

In the recent decades, the KE transfer is downscale. i.e. from ISO to synoptic scales!!! Thus the synoptic scale error may not be actually affecting the ISO time scales.

Rate of kinetic energy exchange (15 year running mean) between ISO and synoptic scale over 60-110E, 5S-27.5N. Positive values indicate that ISO gains Kinetic energy from the synoptic scale

Results (Opportunities)

- The potential predictability of active spells has shown an increase from one week to two weeks while that for break spells increased from two weeks to three weeks.

- The main contribution to the increase in predictability of active/break phases comes from the decrease in initial error or the variance among different ISO events. The ISO phases are becoming more similar.

- The increasing ISO predictability in spite of the decreasing weather predictability was understood from nonlinear kinetic energy exchange studies.

- It shows that in recent decades, the energy transfer is downscale, ie, from ISO to synoptic scale, whereas, prior to 1980s, ISO was drawing energy from synoptic scale.

- It was also found that in recent decades the 30-60 day mode is gaining energy while 10-20 day mode is losing energy and their energy exchange pattern has also undergone a phase reversal. The energized 30-60 day mode may have also favored the increase in potential predictability.

Analysis of the influence of Equatorial Rossby waves on the predictability of ISM active/break spells.

Neena, Suhas and Goswami, 2011, JGR

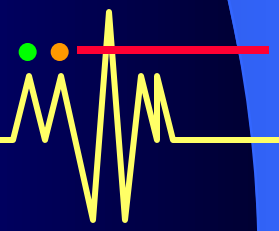

- **Active/beak cycles in monsoon rainfall are brought out by the 30-60 day mode of intraseasonal variability governed by the north south excursions of the ITCZ and are also influenced by the westward propagating 10-20 day ISO mode which originates over either the western Pacific or Bay of Bengal (Krishnamurti and Ardunay, 1980, Chen and Chen 1993).**

- **Another factor in the tropical atmosphere which fall in the same temporal scale and can influence the ISM ISOs are the Equatorial Rossby Waves.**

- **However, not much study has been done to understand the influence of ER waves on ISM variability.**

Observed n=1 ER Variance (wn -10 to -2, eq. depth 10 to 50m)

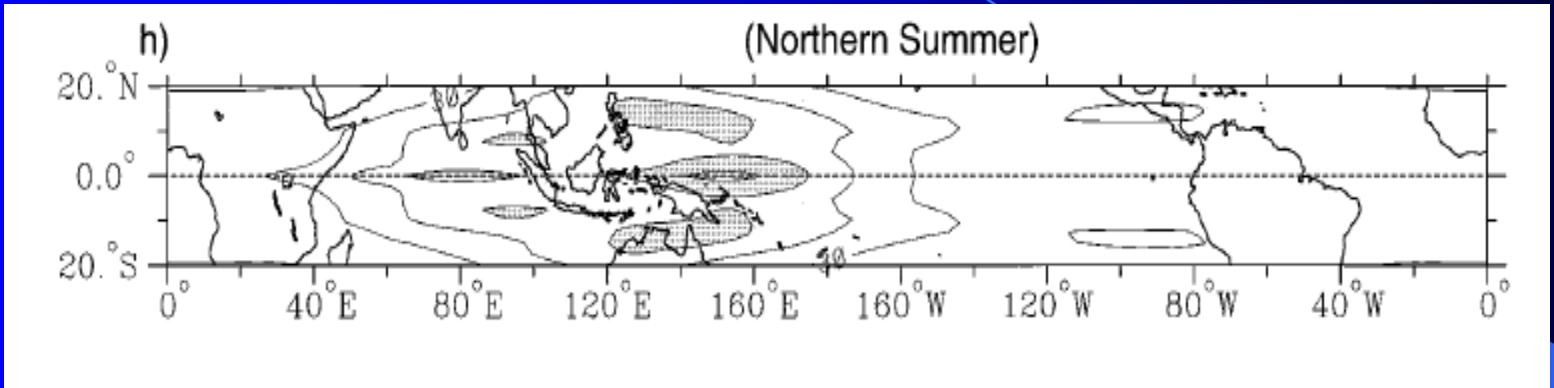

Wheeler and Kiladis, 1999

Centers of activity : eastern IO, western Pacific and eastern Pacific.

The ER waves being dissipative in nature (Masunaga et al, 2007, Hendon and Salby, 1994) it is difficult to identify the signal above the noisy background.

Space time spectra of OLR from 1979-2010

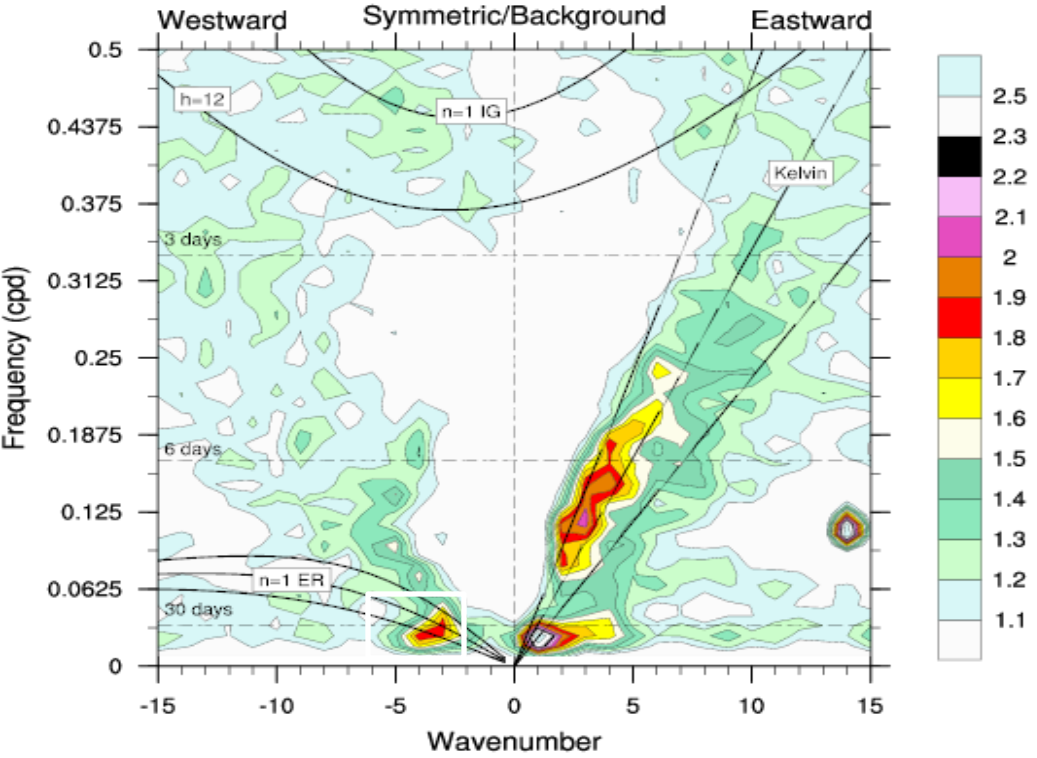

Does this mode have any role in modulating the active/break spells of ISM?

In most studies based on composite, linear regression or EOF based analysis has identified the ER mode over a wide spectral domain (wave number -2 to 10, 10-60 days) **(Kiladis and Wheeler, 1995, Wheeler et al., 2000, Janicot et al., 2010)**.

Thus these studies present an average picture of the waves and fail to notice the existence of high frequency planetary scale modes of the ER wave which are dominant during certain years.

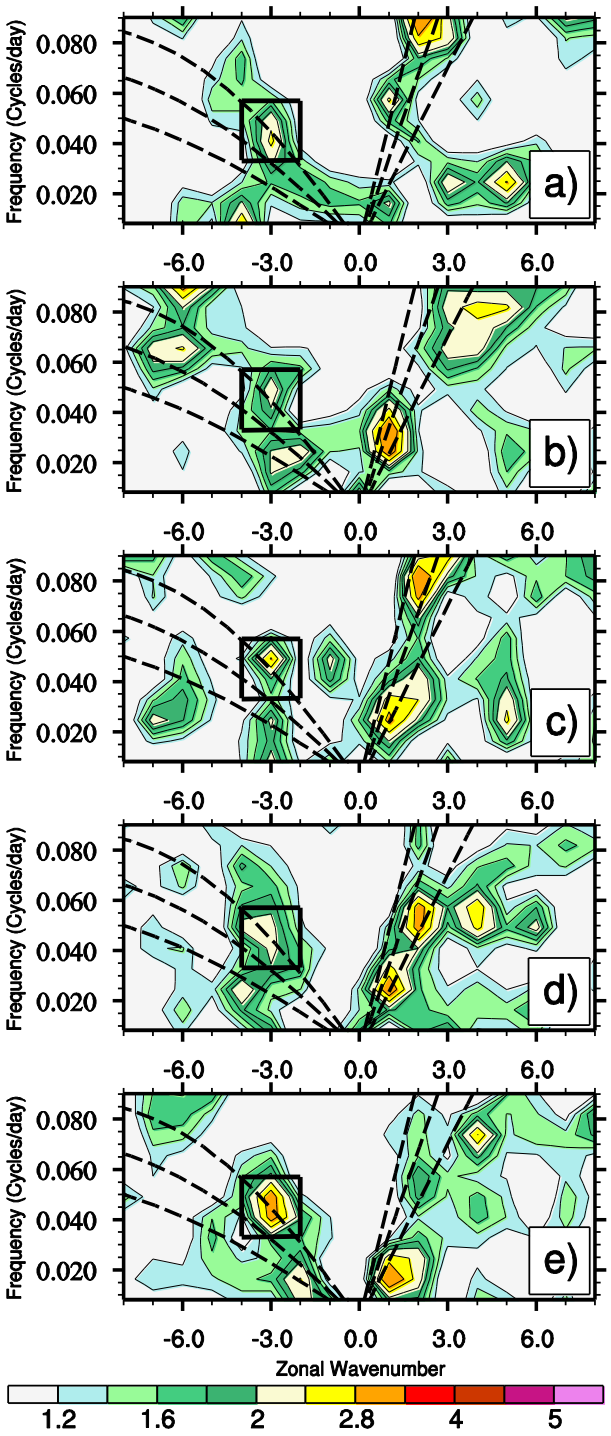

1984

1986

1989

2006

2009

Space time spectra of OLR for the years of high PSER activity around period of 25 days and wave number 3

Large amplitude in the PSER mode is seen during 2009 summer season

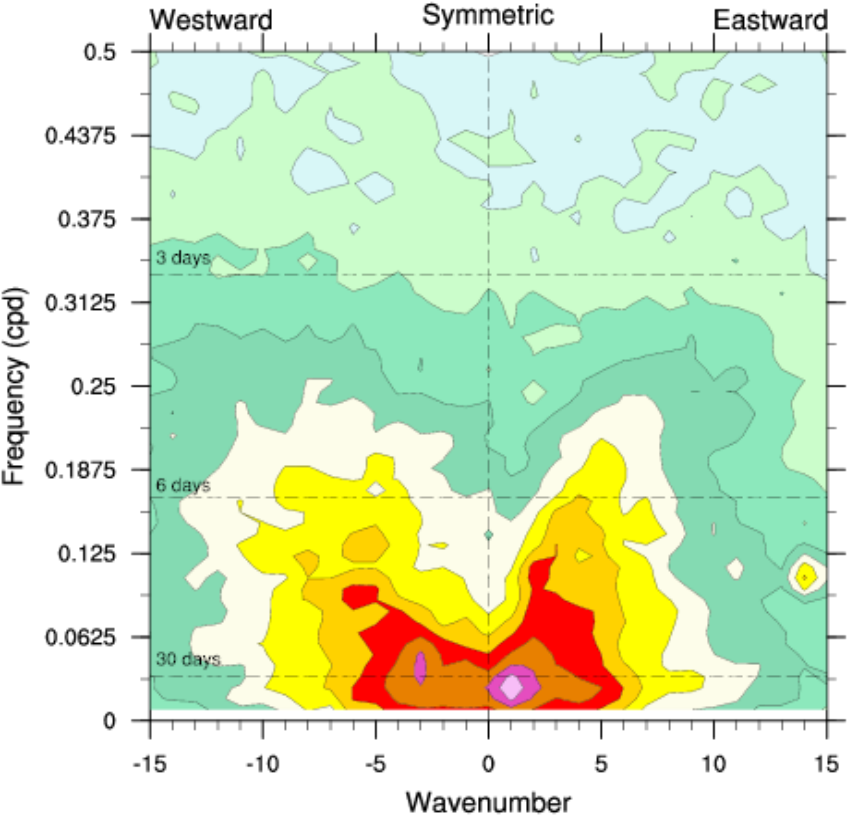

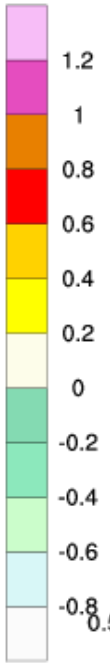

All seven years

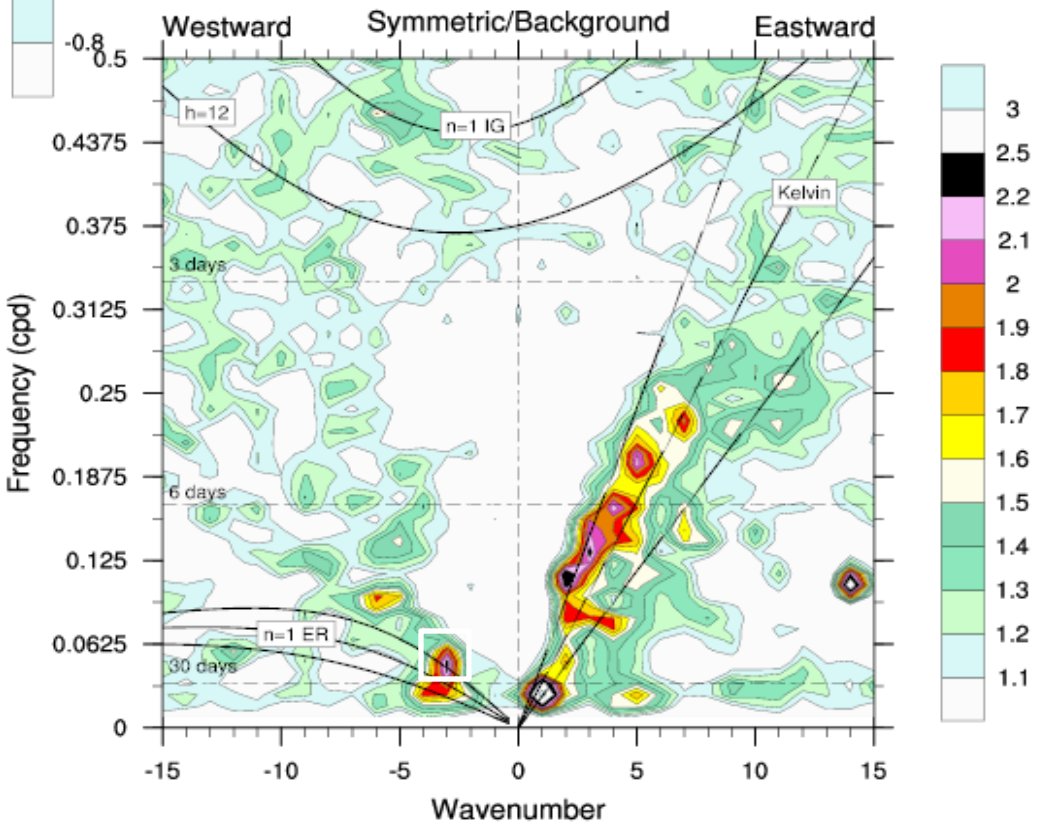

Note the existence of significantly large power in wave number -3, 15-30 day.

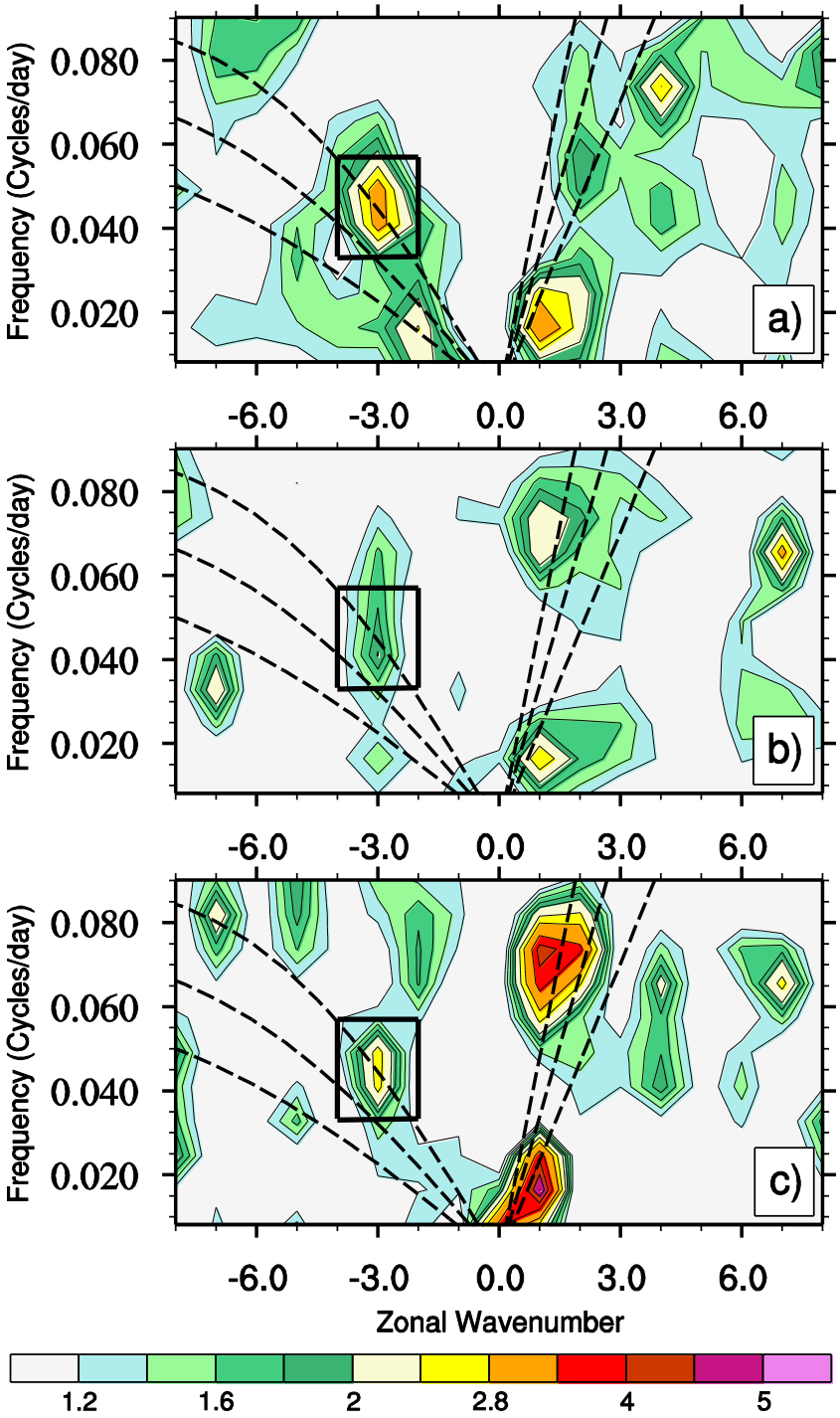

OLR

U850

U200

Symmetric/Background wave number-frequency spectra for JJAS, 2009

Since 2009 exhibits strong ER activity in the planetary scale, we examined the evolution of the PSER mode more closely and investigated its possible influence on the ISM ISOs for the case of 2009 monsoon season.

Power greater than 2.3 is statistically significant at 95% confidence level.

A case to case analysis of the space-time spectra of OLR revealed that during some years, the maximum ER power resides in the **-3 wave number, 15-30 day** region of the spectrum.

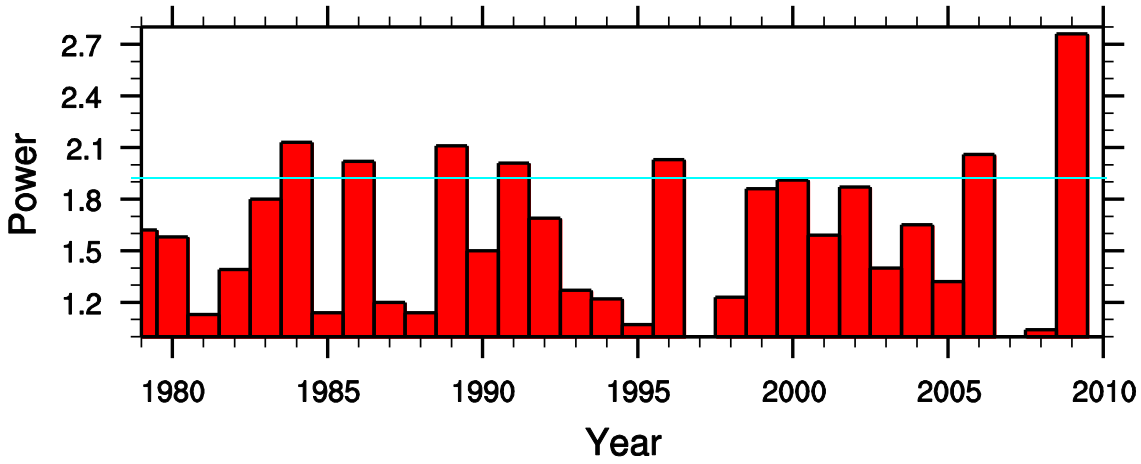

Defining an index (PSER, planetary scale ER) based on the power in this space-time domain, we identified seven seasons **1984, 1986, 1989, 1991, 1996, 2006 and 2009** which exhibited statistically significant (at 10% level) power in the above domain.

Here we investigate whether this PSER mode has a role in modulating the variability and predictability of ISM in intraseasonal and seasonal time scales.

Westward propagating PSER waves during June-August period 2009

Time filtered (15-30 day) OLR anomalies.

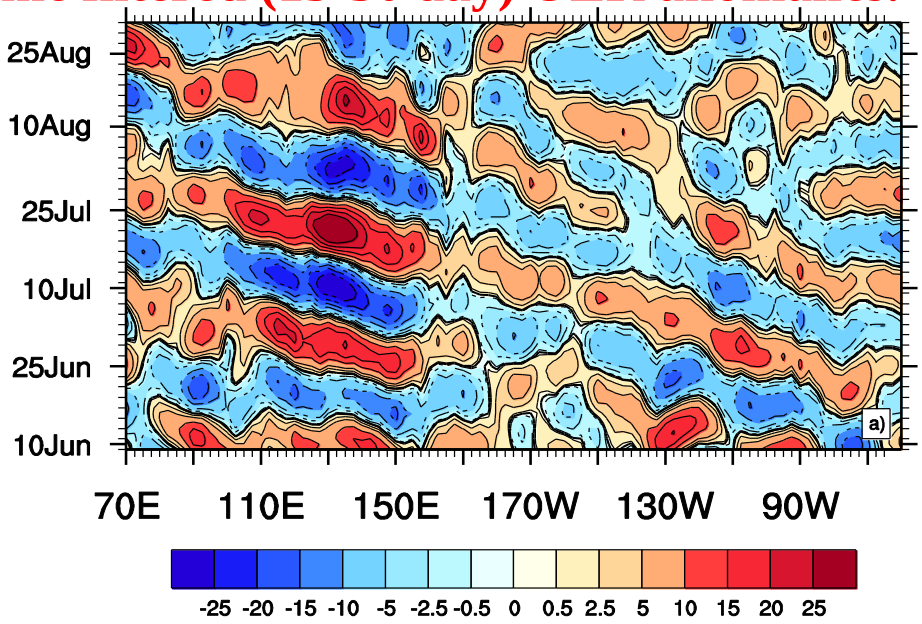

The PSER waves originate over the eastern Pacific in third week of June, propagate westward at a speed of about 6m/s and reach the ISM domain by third week of July.

Unfiltered OLR anomalies overlaid with space time filtered OLR anomalies.

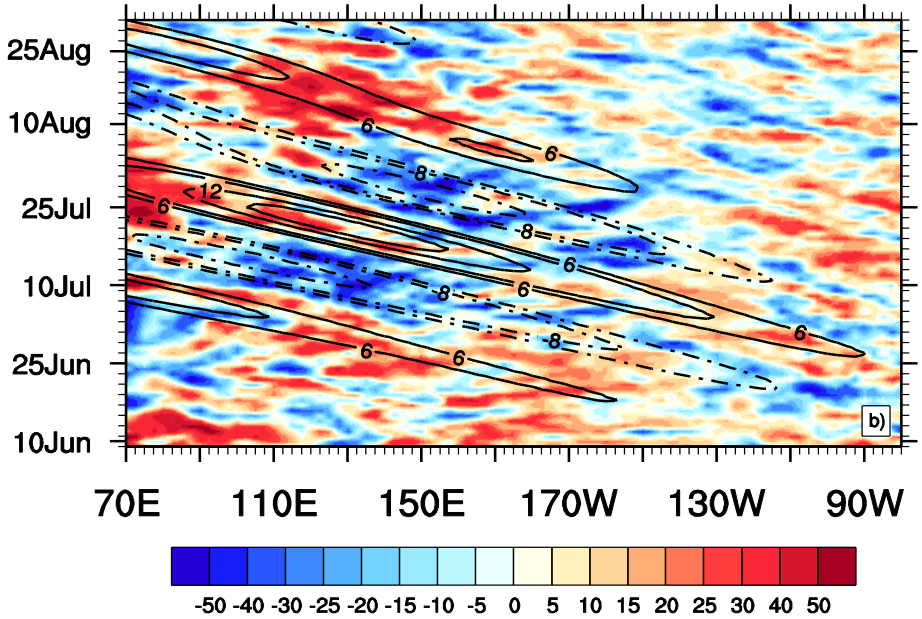

It may be noted that the PSER activity does not sustain throughout the season, but is rather transient.

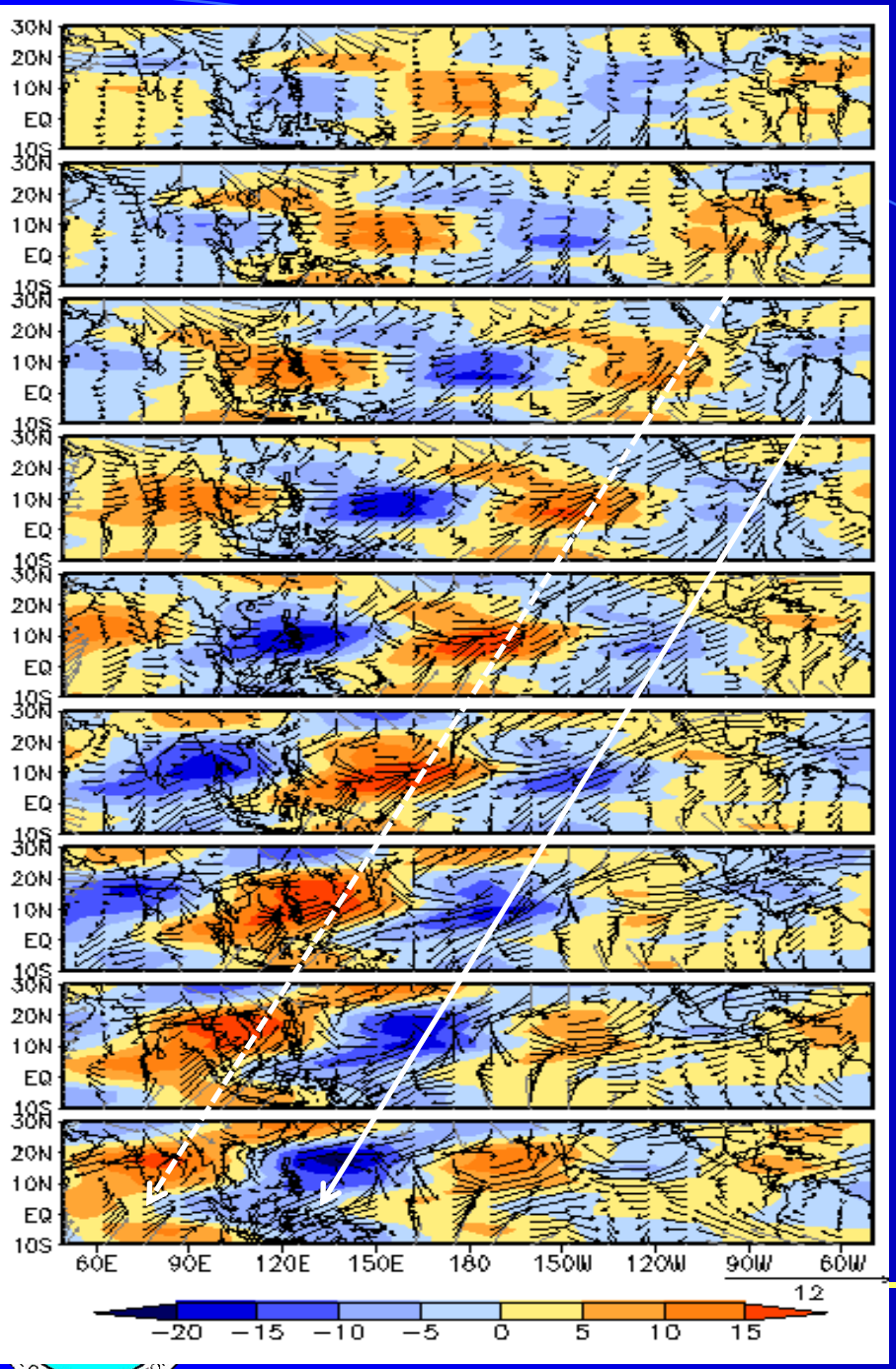

Five day averages of space-time filtered (PSER) OLR and wind anomalies at 200 hPa, starting from 21 June 2009.

Westward propagation of active (suppressed) convection is shown by solid (dotted) line.

Spatial structure of PSER wave - 2009 case

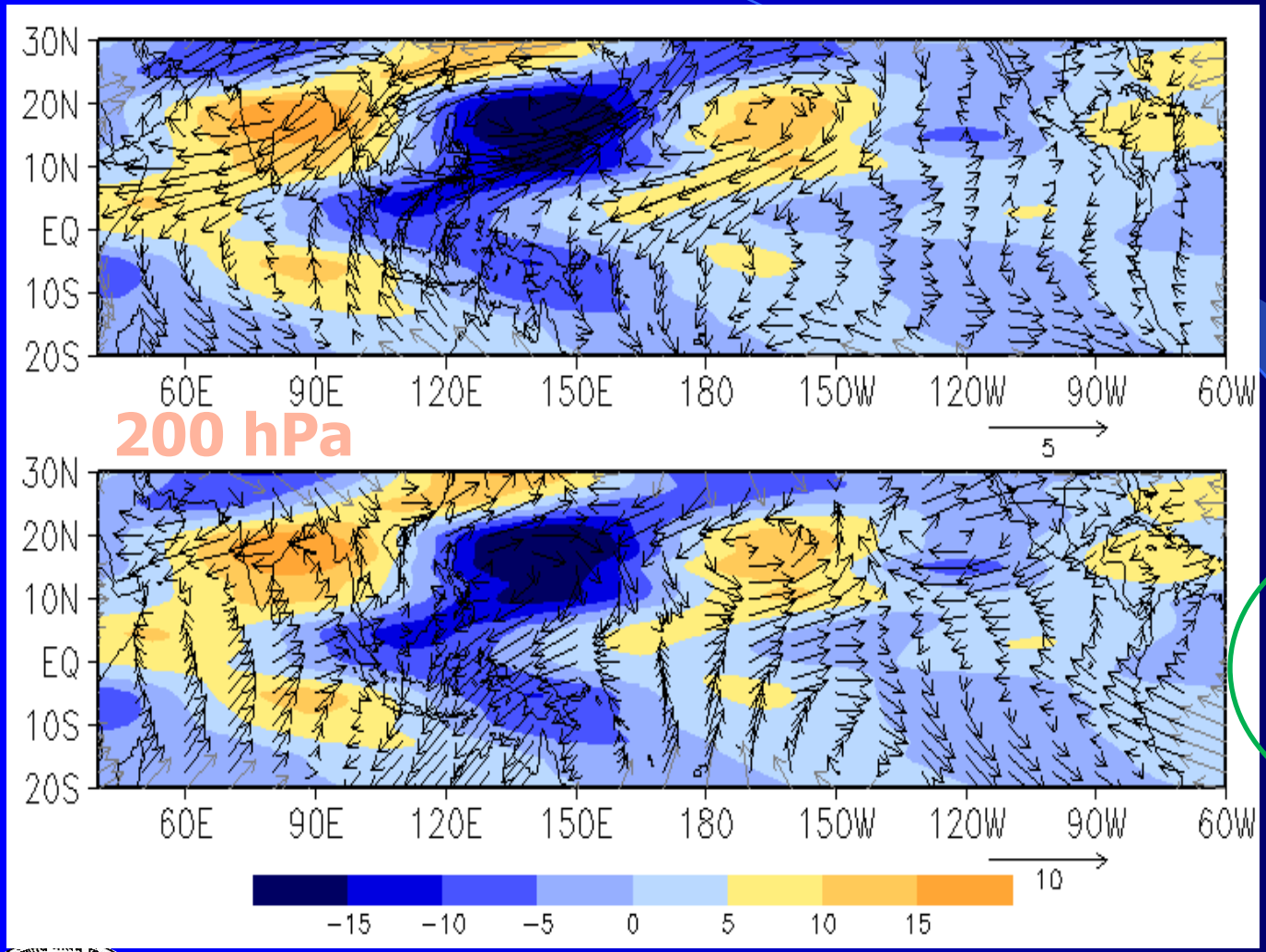

Space time filtered anomalies of OLR (shaded) and wind (vectors).

August 1

The mode exhibit a n=1 baroclinic structure

- The transient behavior of PSER waves raises the question of what forces the waves?

- Eastward propagating ISO of large amplitude can trigger westward propagating ER modes either through modulation of convective anomalies or through interaction with north-south oriented mountain ranges on the west coast of America. The preferable spatial and temporal scales of such ER waves may also be altered through interactions (Roundy and Frank, 2004).

- Westward propagating ER modes may also arise from decoupling of the MJO Kelvin Rossby couplet (Hayashi and Sumi, 1986).

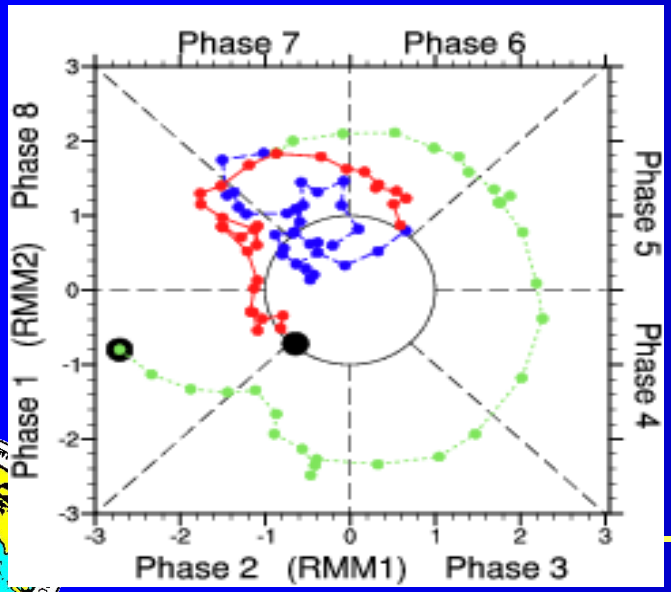

- RMM1-RMM2 phase space shows that the MJO activity was weakening over the eastern Pacific at the time of generation of the PSER mode.

- This implies a possible association of the PSER mode with the decoupling of MJO.

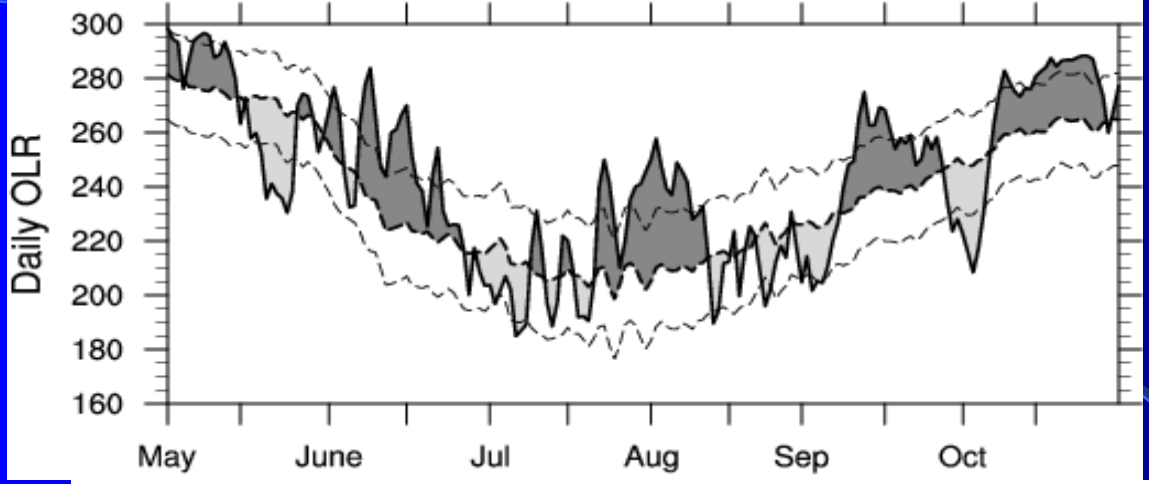

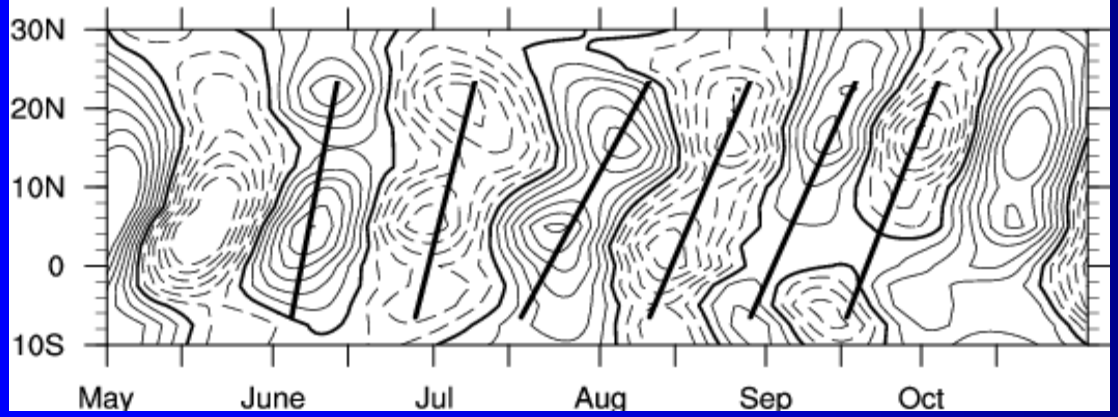

The ISM domain

Northward propagating 30-90 day mode

Solid contours --- positive anomalies

dashed contours -- negative anomalies.

It is known that the ISM domain experienced a long break condition from third week of July to second week of August.

We hypothesize that arrival of the divergent phase of the PSER mode over the ISM domain by the end of July might have significantly modulated the monsoon ISO and lead to the extended break condition.

Nonlinear KE exchange between 15-30 day scale and 60 day scale at 850 hPa.

KE exchange is calculated using 60 day sliding window starting from 1April 2009

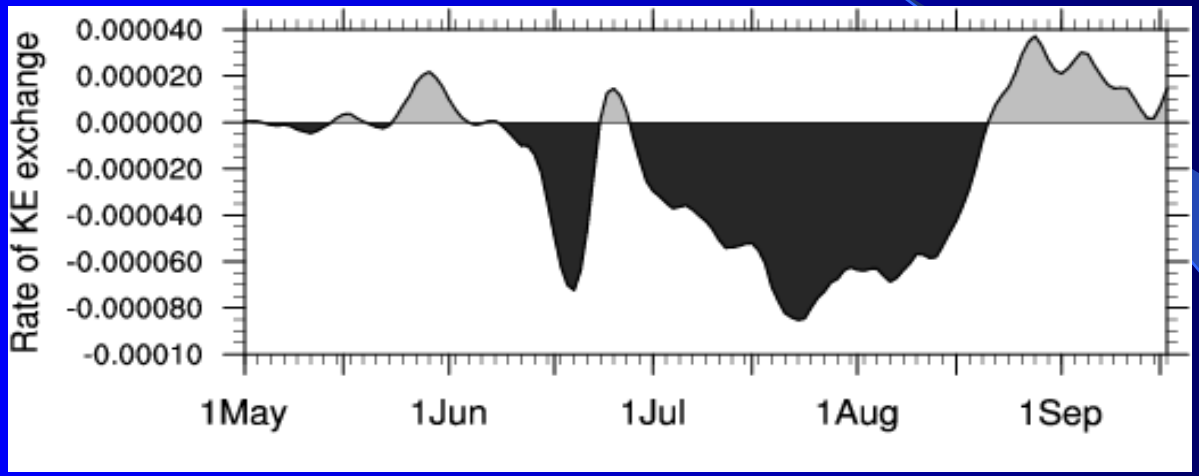

Rate of KE exchange per unit mass (W/kg).

Negative values indicate the flow of KE from 15-30 day to 60 day scale.

The abscissa represents the middle date corresponding to each sliding window.

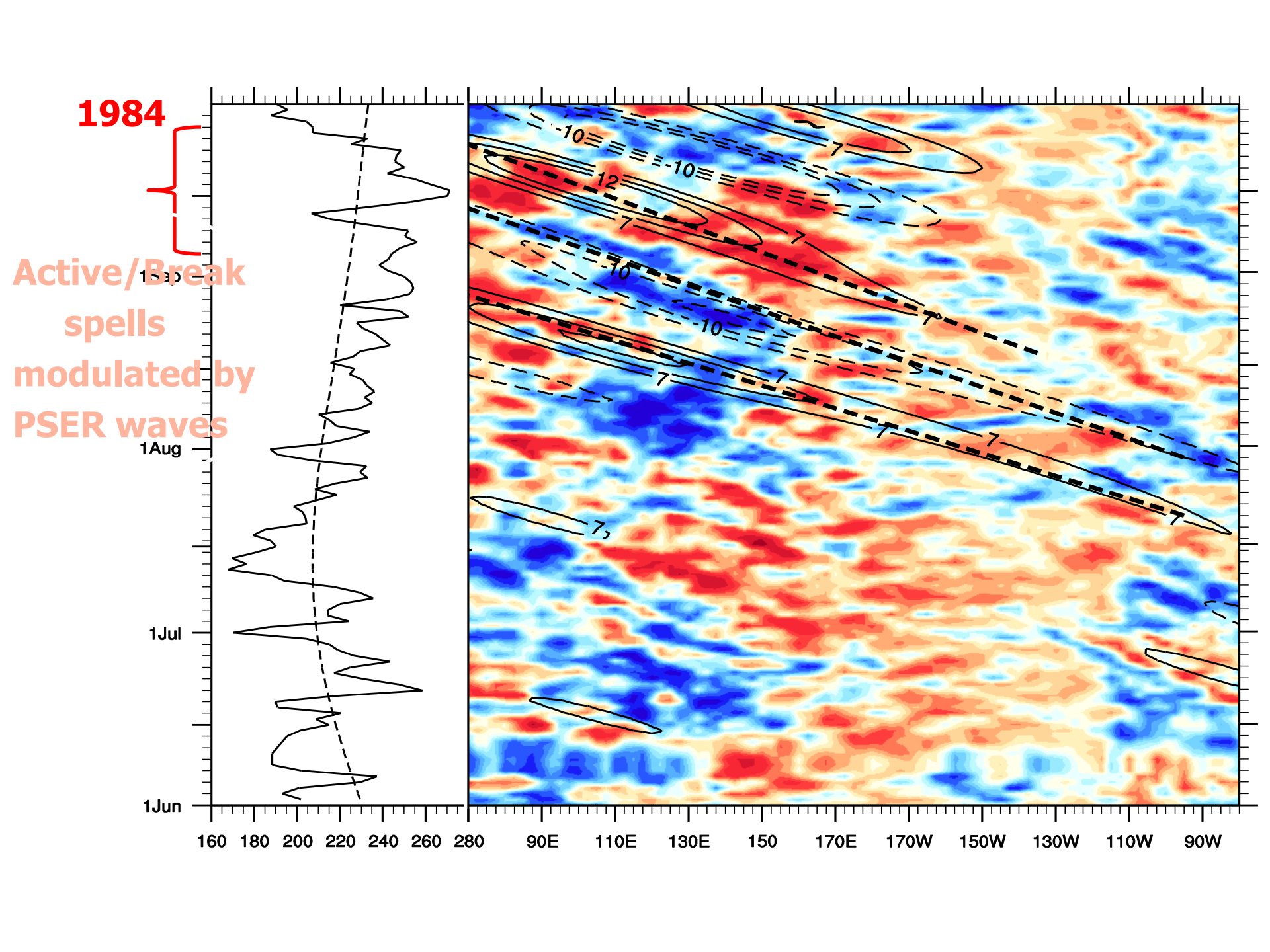
1984
Active/Break spells modulated by PSER waves
1Aug
1Jul
1Jun
160 180 200 220 240 260 280
90E 110E 130E 150 170E 170W 150W 130W 110W 90W
-10
12
7
10

Unfiltered OLR anomalies and space time filtered OLR anomalies

1986

Active/Break spells modulated by PSER waves

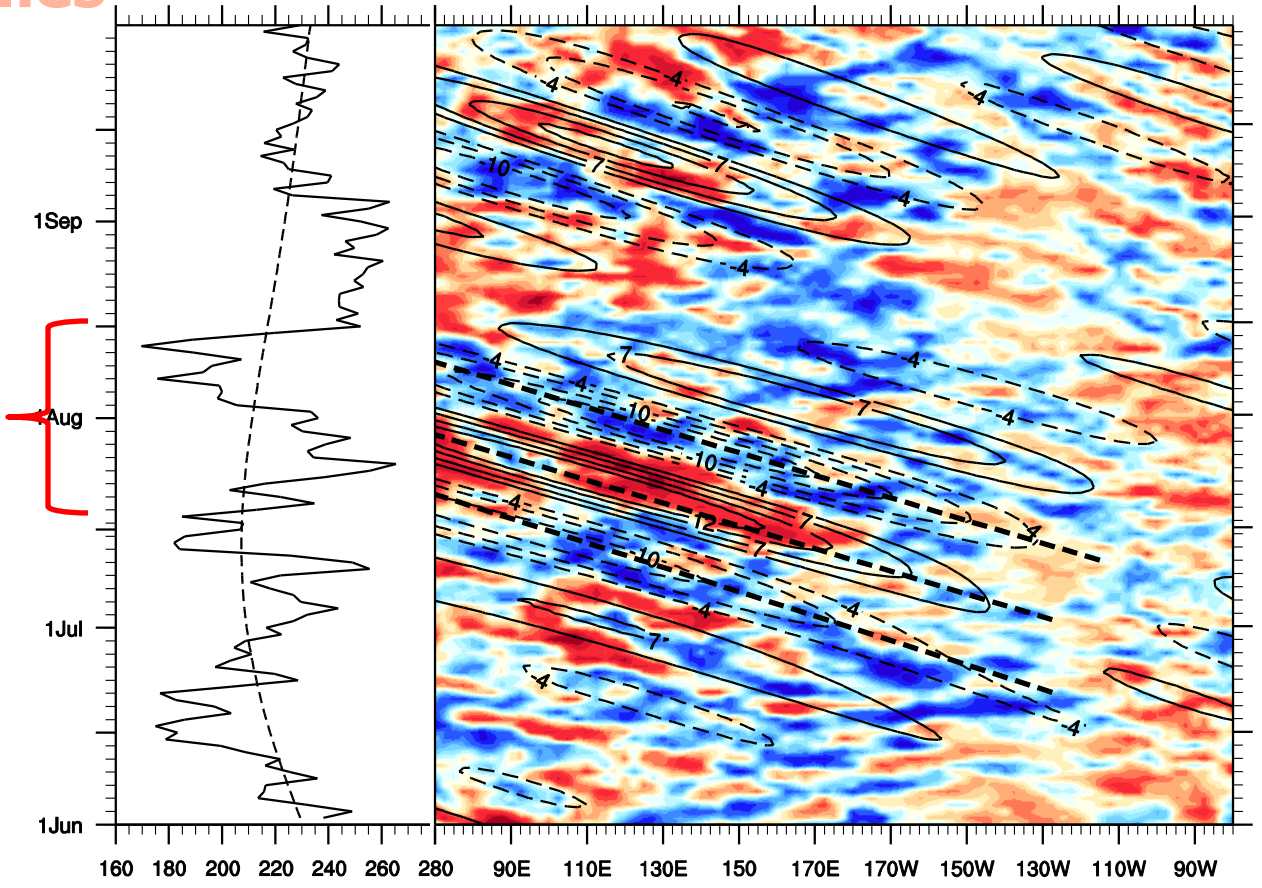

Area averaged over
10N-25N
70E-82.5E

Averaged over
0-20N

Clim Dyn
DOI 10.1007/s00382-010-0971-3

Absorbing aerosols facilitate transition of Indian monsoon breaks to active spells

M. G. Manoj · P. C. S. Devara · P. D. Safai · B. N. Goswami

Aerosol and Mean Indian Monsoon

- Surface cooling of continent, weakening NS temp gradient and weakening of monsoon
- Elevated Heat Pump Mechanism
  - Strengthening of the monsoon

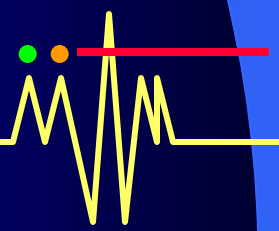

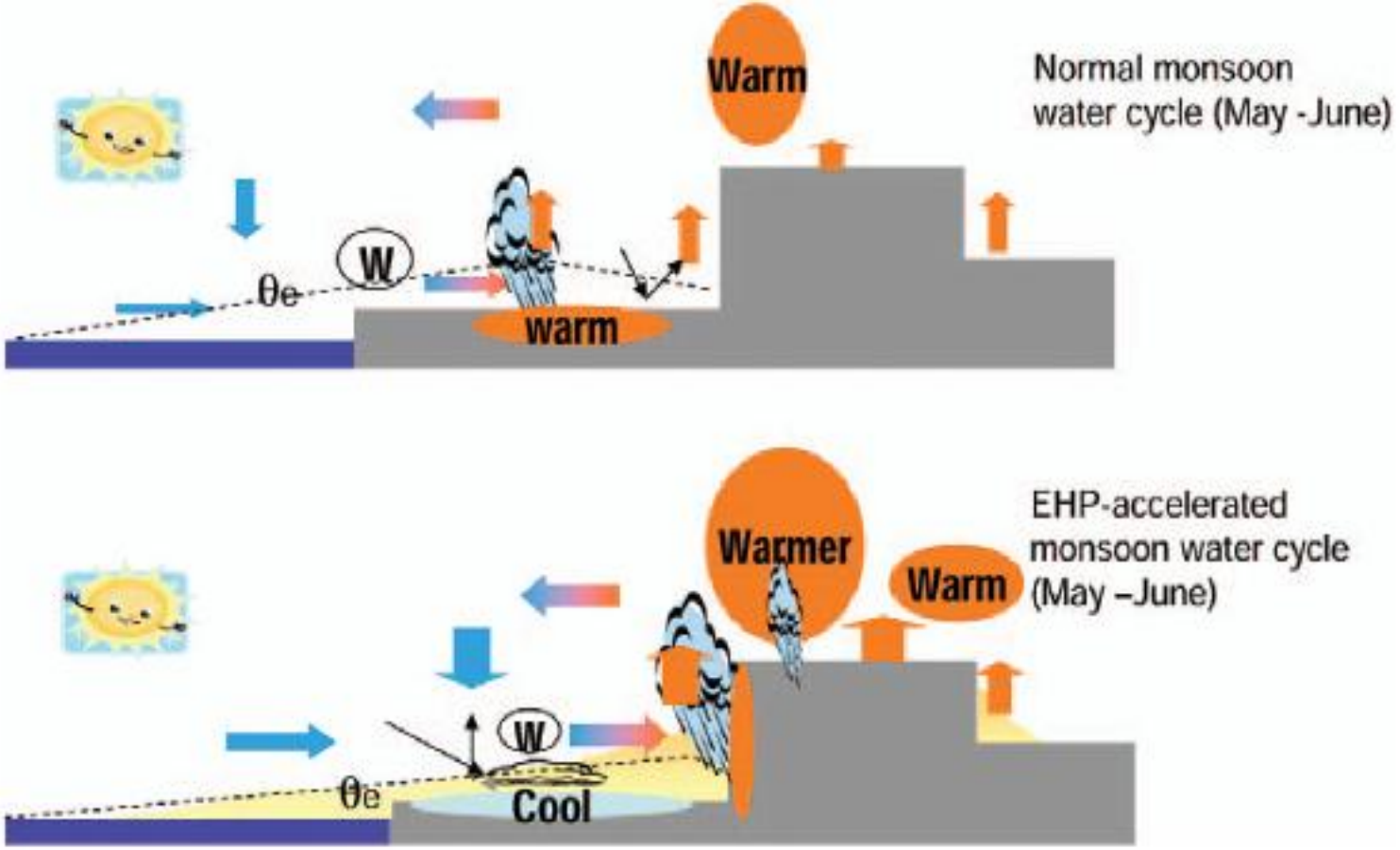

FIG. 3. Schematic showing the monsoon water cycle (top) with no aerosol forcing and (bottom) with aerosol-induced elevated heat pump effect. Low-level monsoon westerlies are denoted by W. The dashed line indicates magnitude of the low-level equivalent potential temperature θ_e. Deep convection is indicated over regions of maximum θ_e. (See text for further discussions.)

EHP

Lau et al

Aerosols Influence Monsoon ISOs

- While there has been some studies to address the influence on the seasonal mean monsoon, no study has so far addressed how aerosols may influence the MISO
- Do we expect the aerosols to influence MISO?

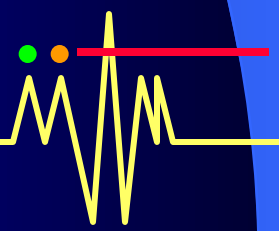

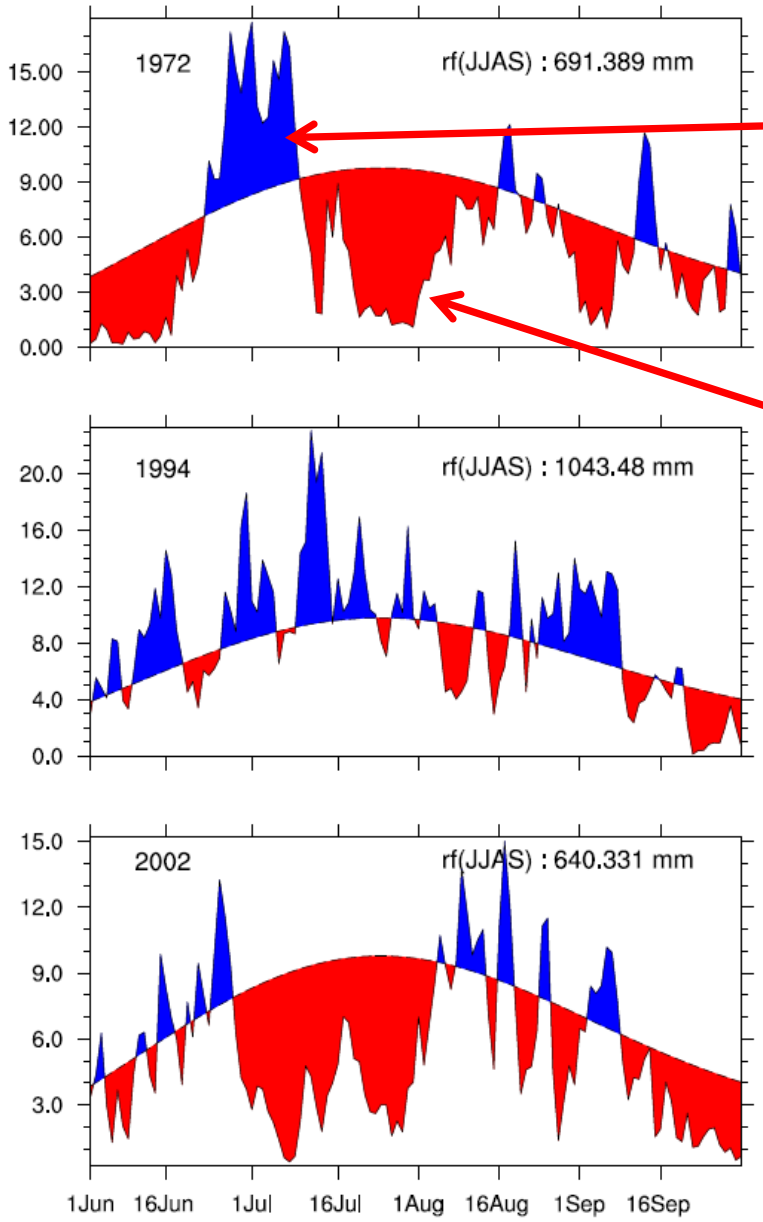

Active

Break

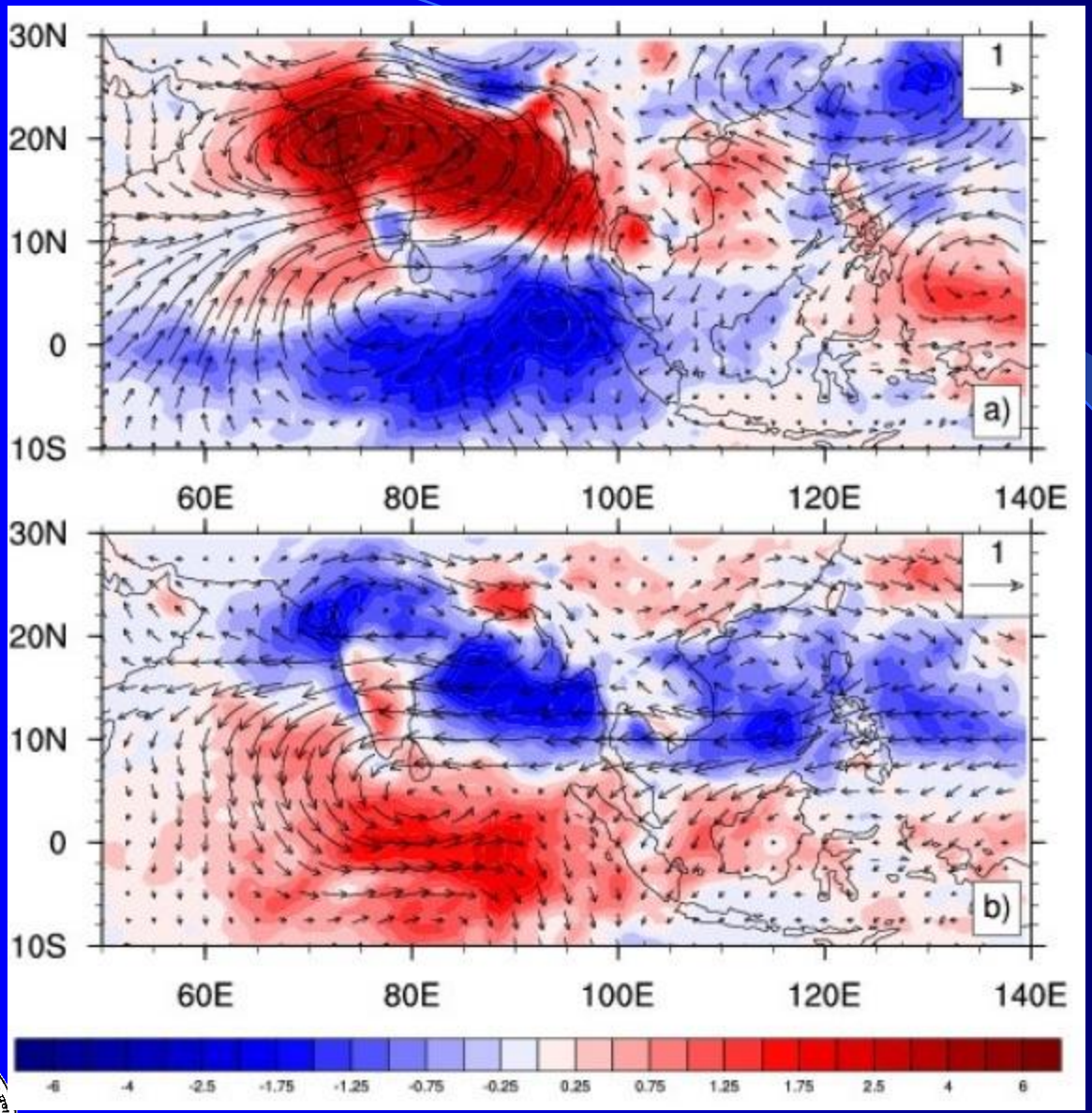

Precip and wind anom during Active

Precip and wind anom during Break

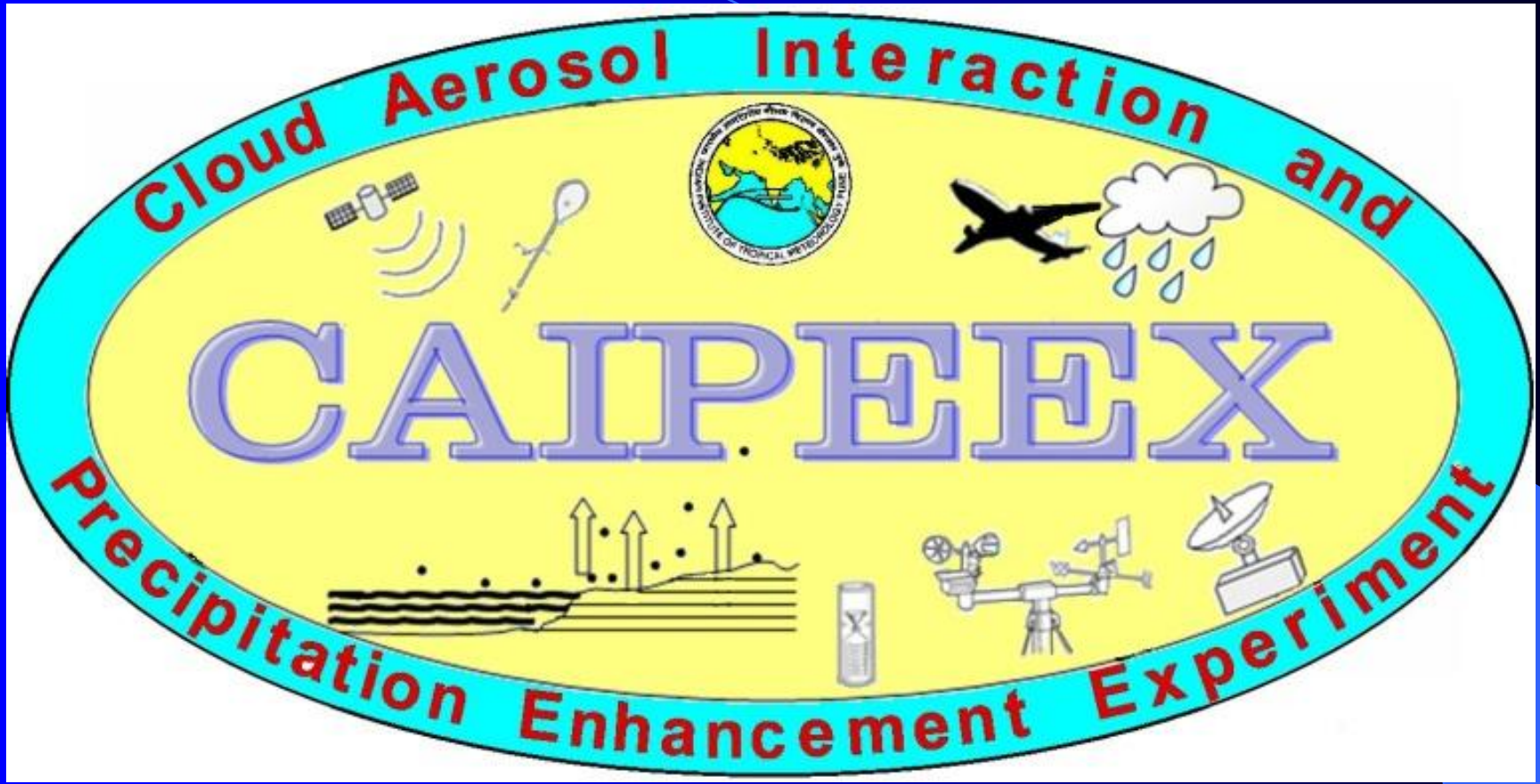
Cloud Aerosol Interaction and
CAIPEEX
Precipitation Enhancement Experiment

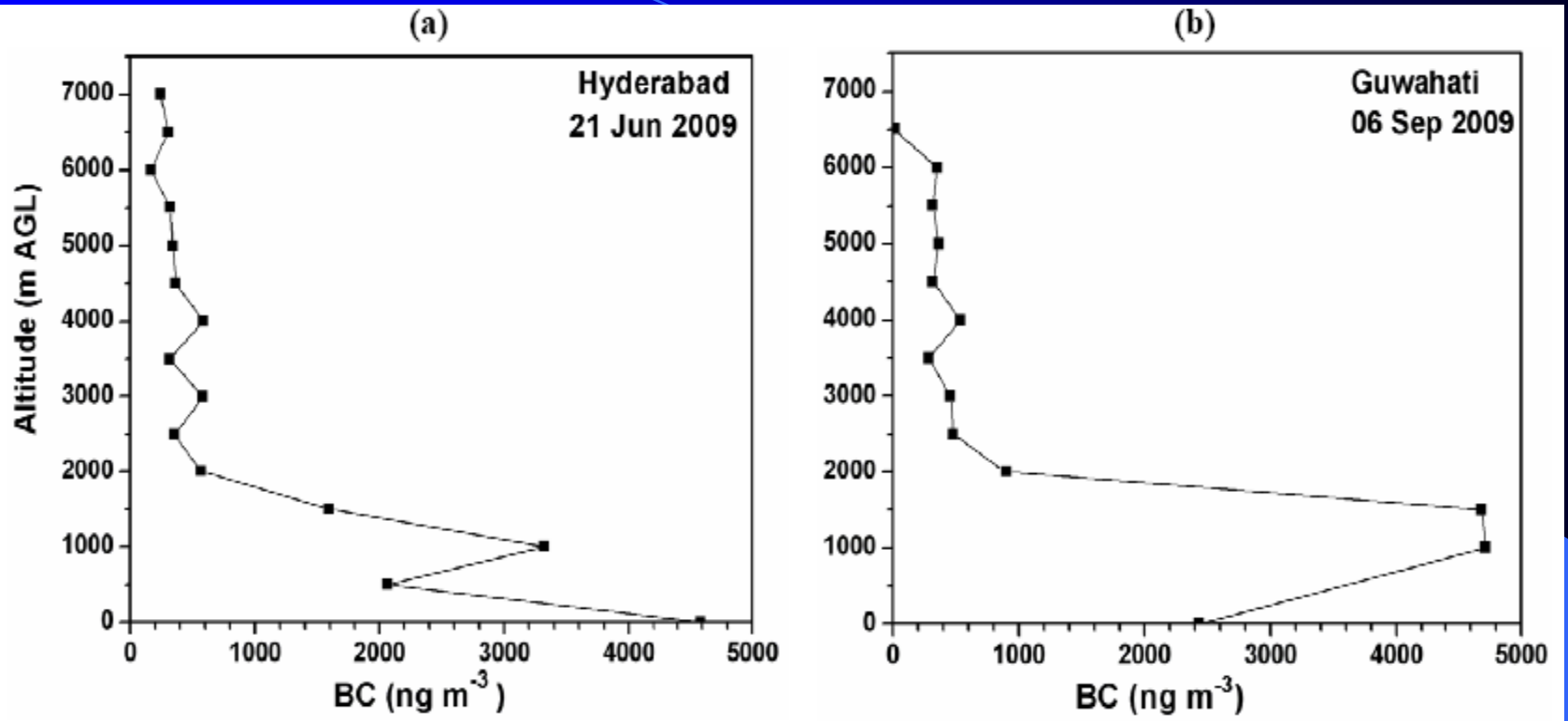

Fig. 1 Vertical profile of black carbon aerosol measured by an Aethalometer during CAIPEEX Phase-I. Significant loading of BC between 1-3 km is seen over the stations **(a)** Hyderabad in central India on June 21, 2009 and **(b)** Guwahati in north-east India on September 06, 2009.

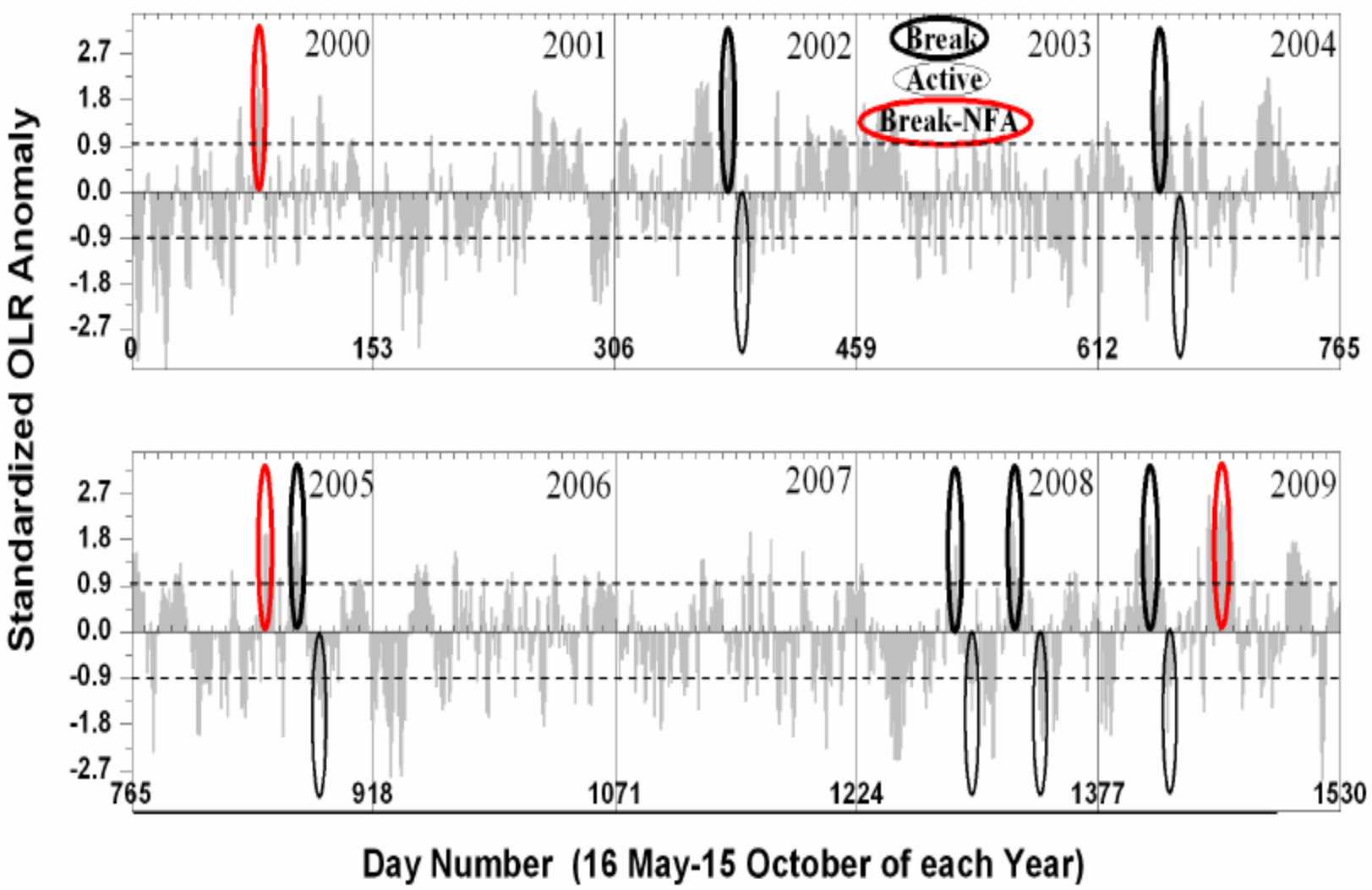

Fig. 2 Standardized OLR anomalies for the period 2000-2009. Long break cycles (thick black solid circles) followed by active spells (thin black circles) together with those breaks immediately not followed by active episodes (thick red circles).

AOD, Break

BFA

AOD Anom Break

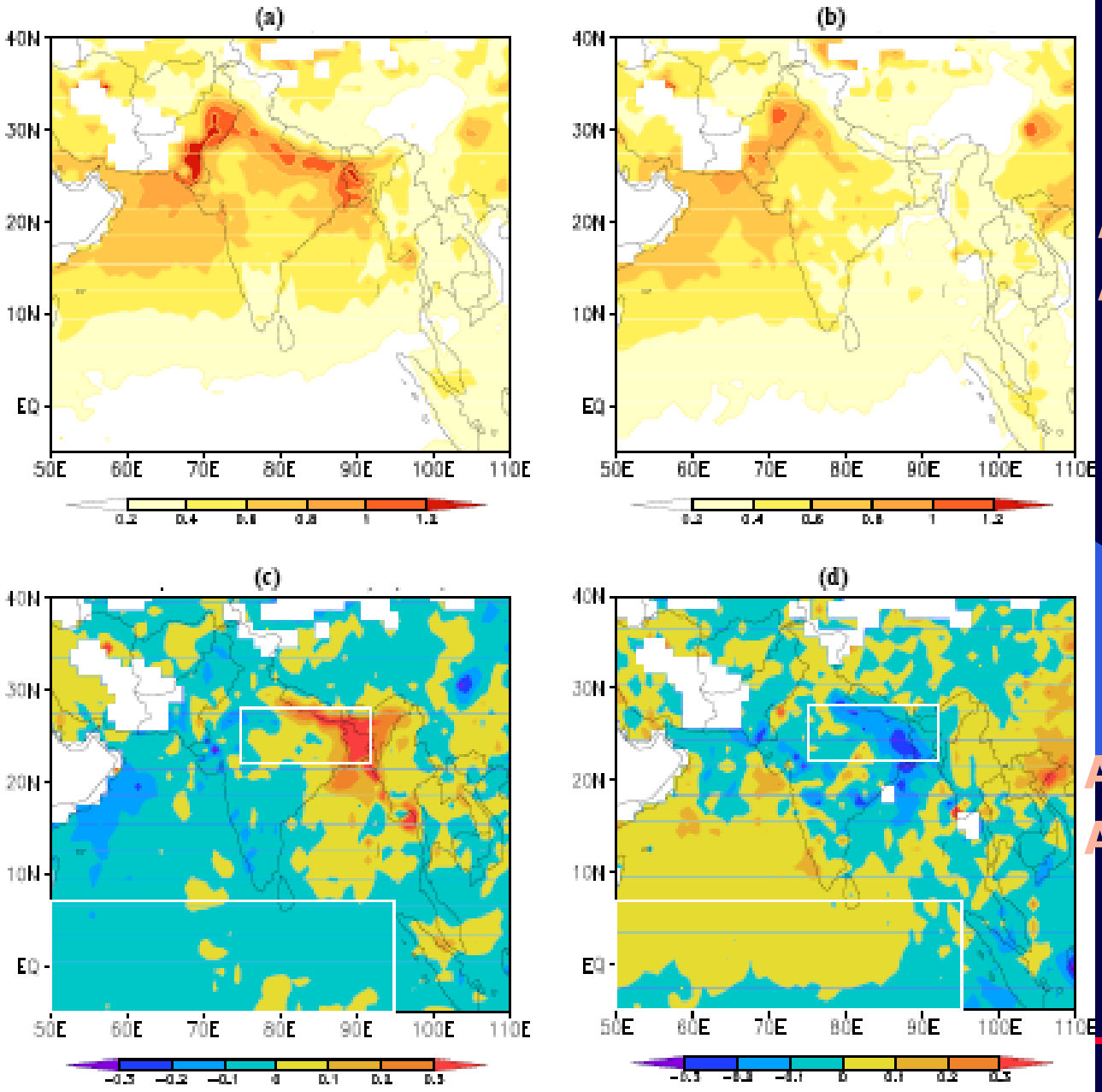

AOD, Active

AOD Anom Active

Fig. 4 Composite of actual AOD at 550 nm during BFA cases: (a) breaks (b) actives. Composite of AOD anomaly at 550 nm during (c) breaks (d) actives.

AI Break

BFA

AI Break-Active

AI Active

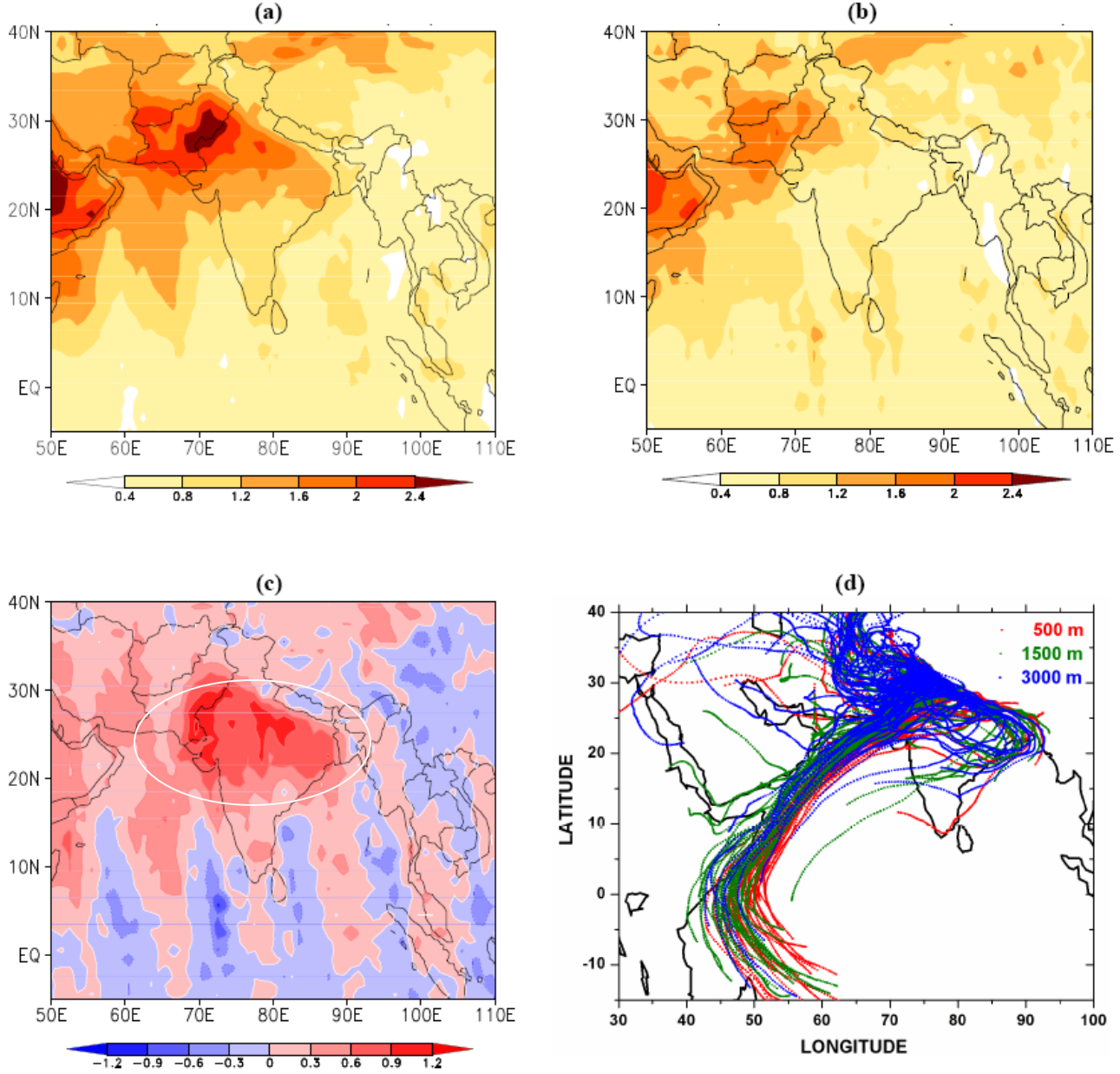

Fig. 5 Composite Aerosol Index during BFA cases: **(a)** breaks **(b)** actives **(c)** break minus active and **(d)** breaks composite of seven-day back-trajectories ending at 0000 UTC at the receptor point (80°E; 28°N) over the Indo-Gangetic Plain for the altitudes 500, 1500 and 3000 m.

AOD-BNFA

AOD-BFA-BNFA

AI-BNFA

AI-BFA-BNFA

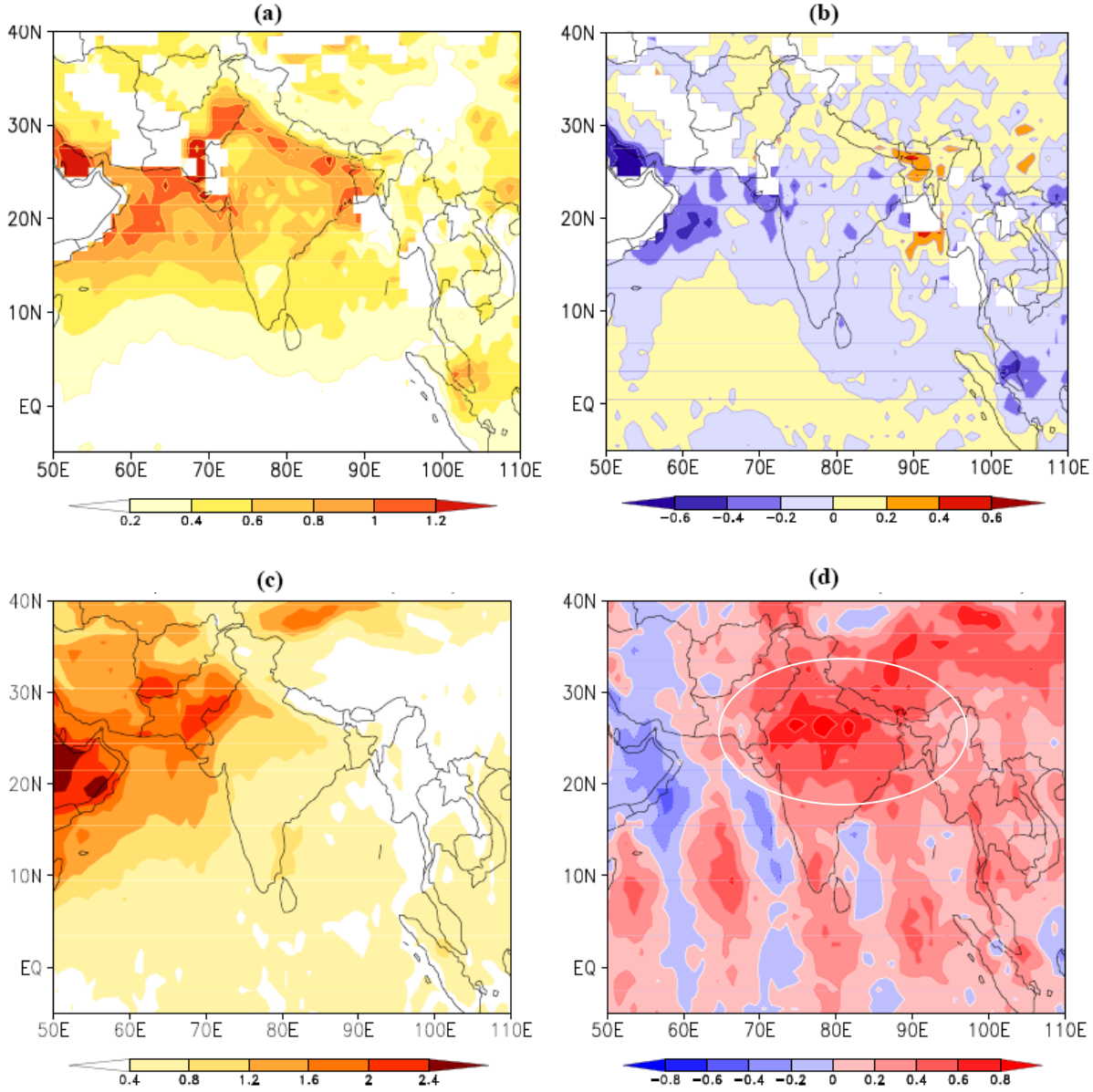

Fig. 7 Composite of actual AOD at 550 nm and Aerosol Index during BNFA and their difference with corresponding BFA break cases. **(a)** AOD (BNFA) **(b)** AOD (BFA minus BNFA) **(c)** AI (BNFA) and **(d)** AI (BFA minus BNFA)

INDIAN INSTITUTE OF TROPICAL METEOROLOGY PUNE

(c)

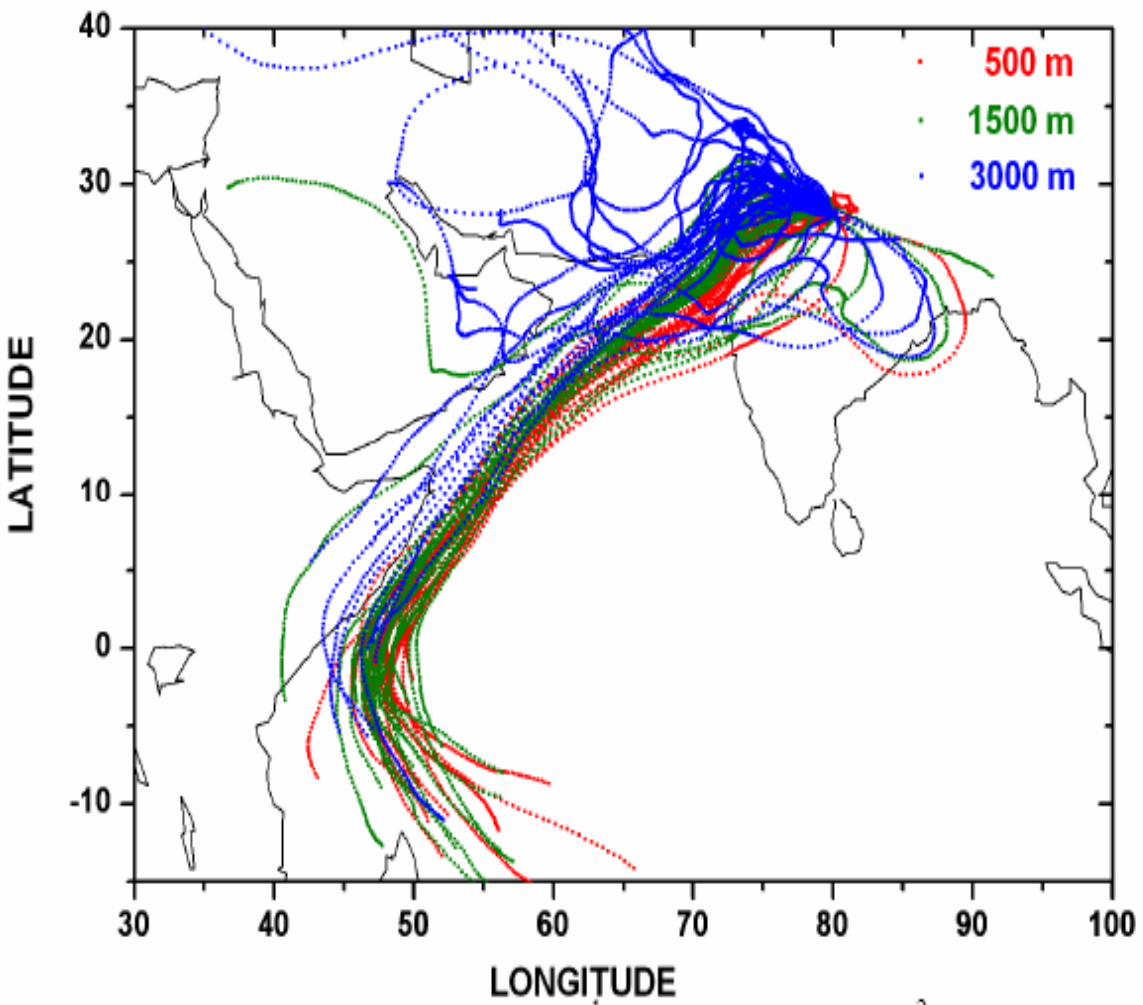

Fig. 8: Composite anomalies of **(a)** 850 hPa wind in ms^{-1} and **(b)** OLR in Wm^{-2} during BNFA cases. **(c)** Back-trajectories ending at 0000 UTC at the receptor point (80°E; 28°N) at three height levels during BNFA.

Break

Active

BFA

Winds

OLR

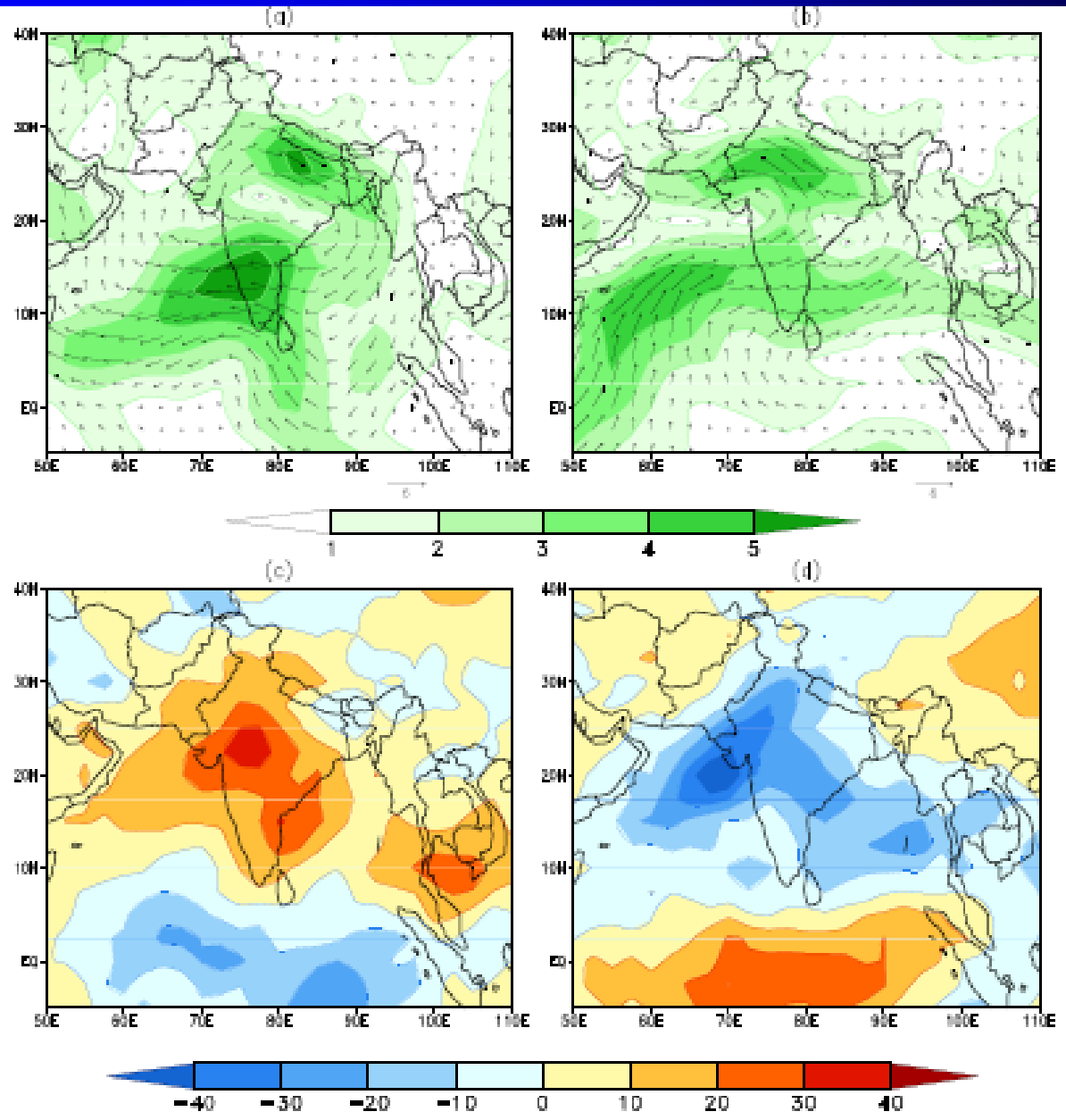

Fig. 3 Composite of circulation anomalies in ms^{-1} during BFA cases: (a) breaks (b) actives. (c) and (d) are same as (a) and (b) respectively, but for OLR anomalies in Wm^{-2}.

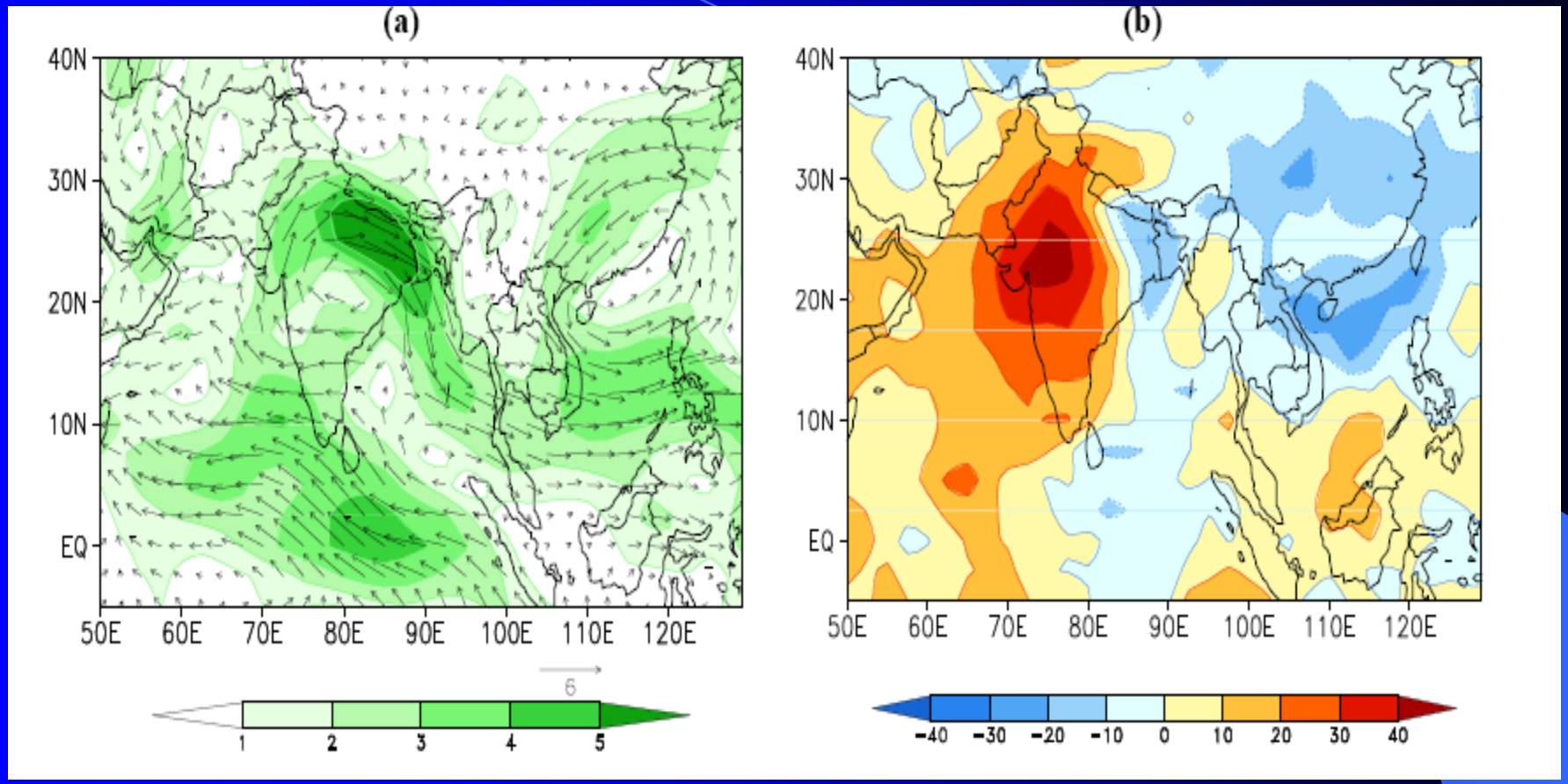

850 hPa wind anom
BNFA

OLR anom
BNFA

Hypothesis

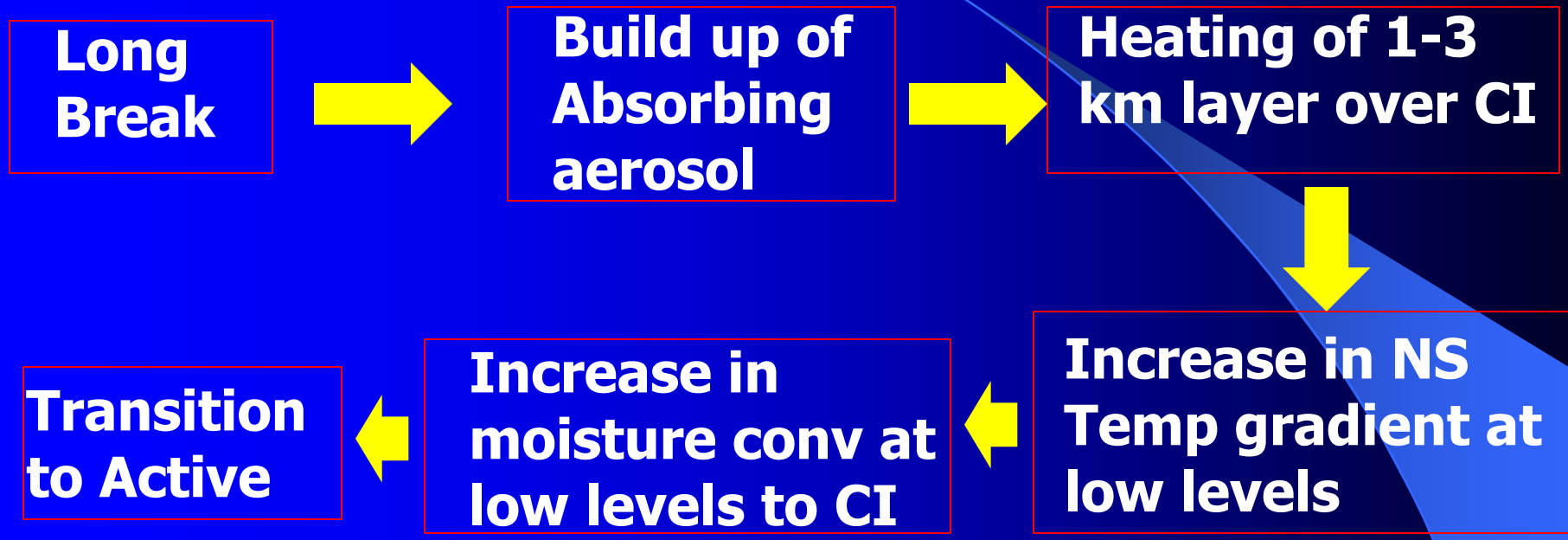
Long Break
Build up of Absorbing aerosol
Heating of 1-3 km layer over CI
Increase in NS Temp gradient at low levels
Increase in moisture conv at low levels to CI
Transition to Active

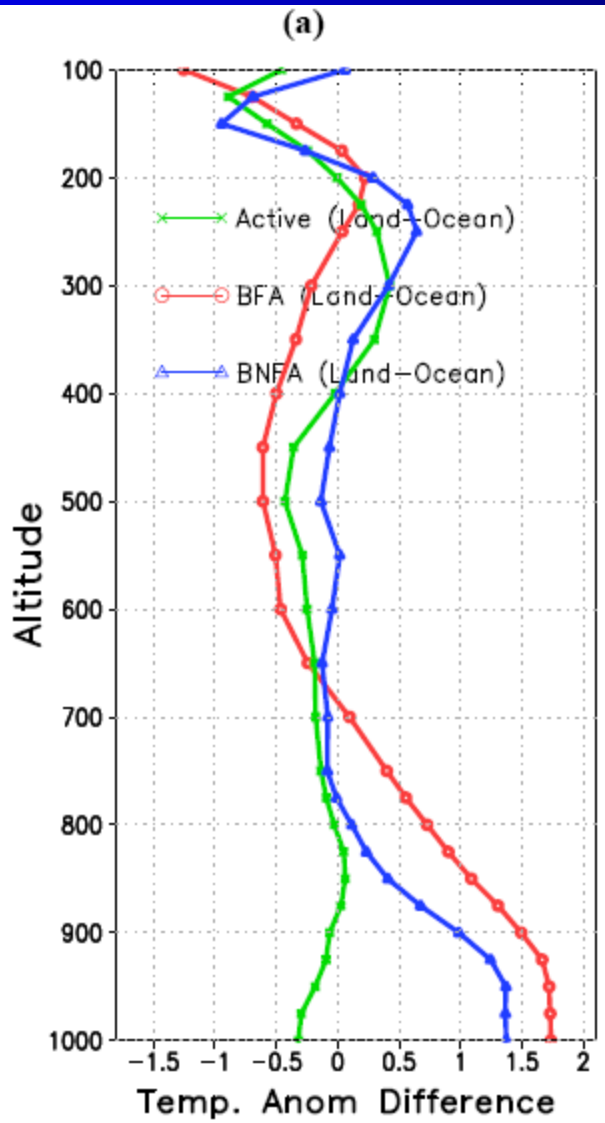

Fig. 6 (a) Vertical profile showing difference of temperature anomalies (Land minus Ocean) in °C during BFA breaks, actives and BNFA spells.

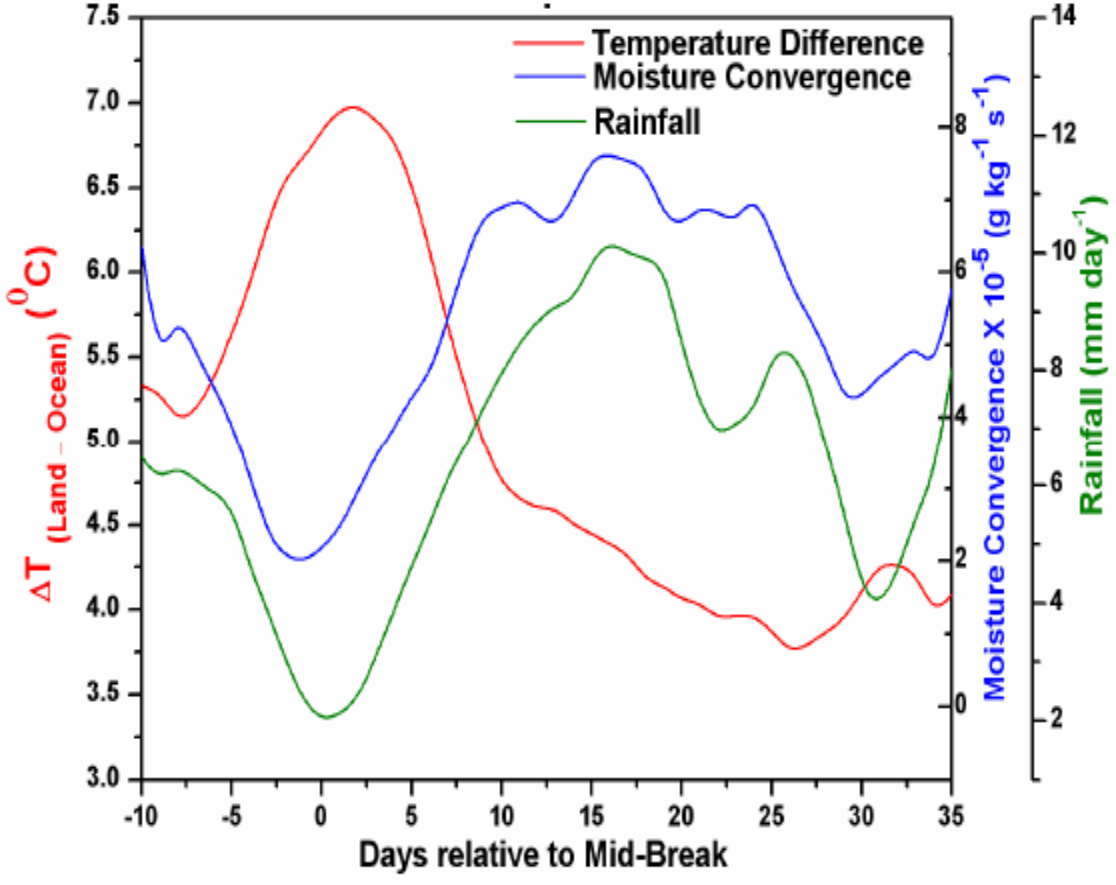

Fig. 6 (b) Composites of time evolution of temperature difference at 925 hPa between Land and Ocean, moisture convergence at the same level and rainfall w.r.t. the mid-day of BFA breaks composite.

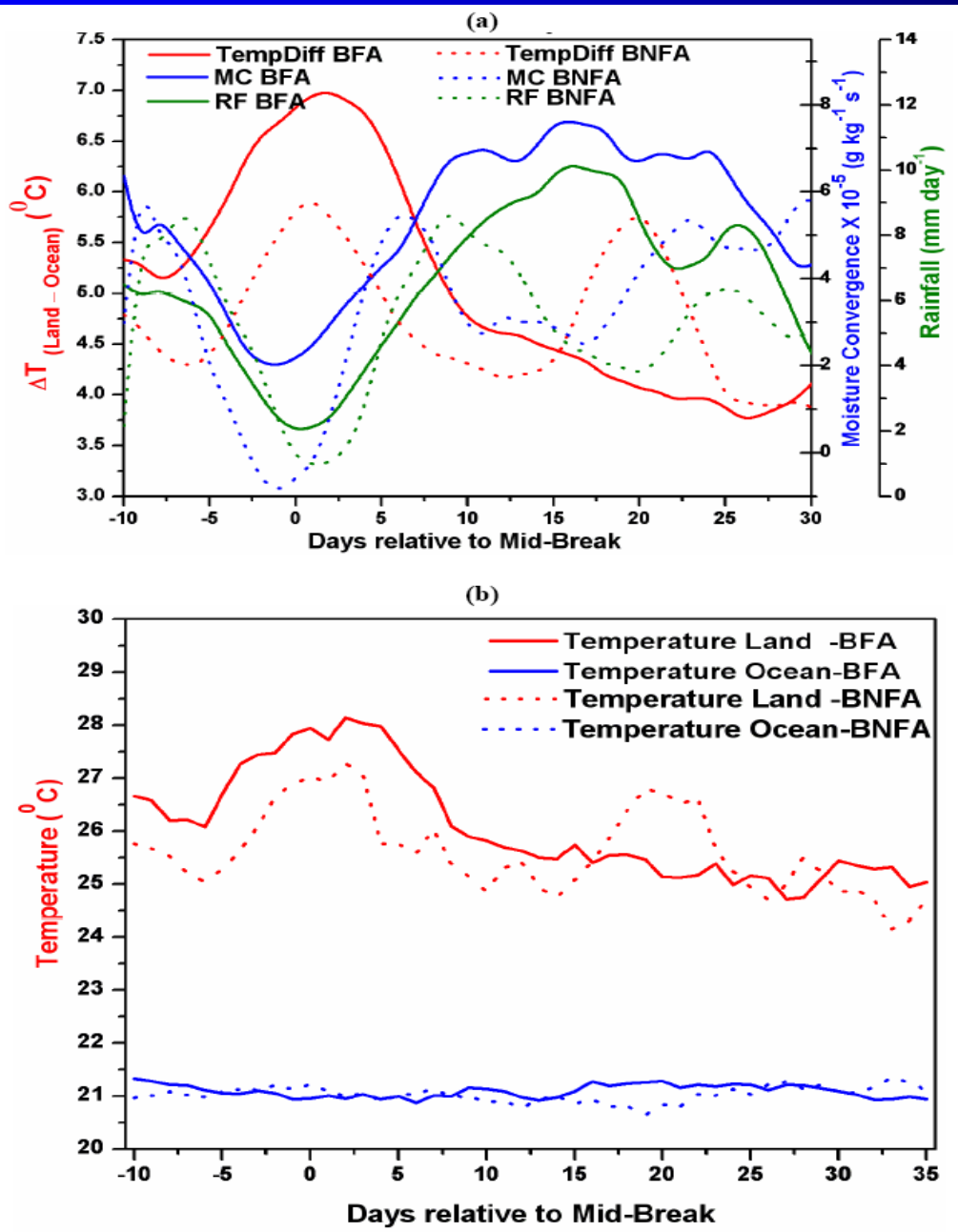

Fig. 9: (a) Composites of time evolution of temperature difference at 925 hPa between Land and Ocean, moisture convergence and rainfall w.r.t. the mid-day of BFA breaks and BNFA composites **(b)** Time evolution of actual temperature at 925 hPa over Land and Ocean w.r.t. the mid-day of BFA breaks and BNFA composites.

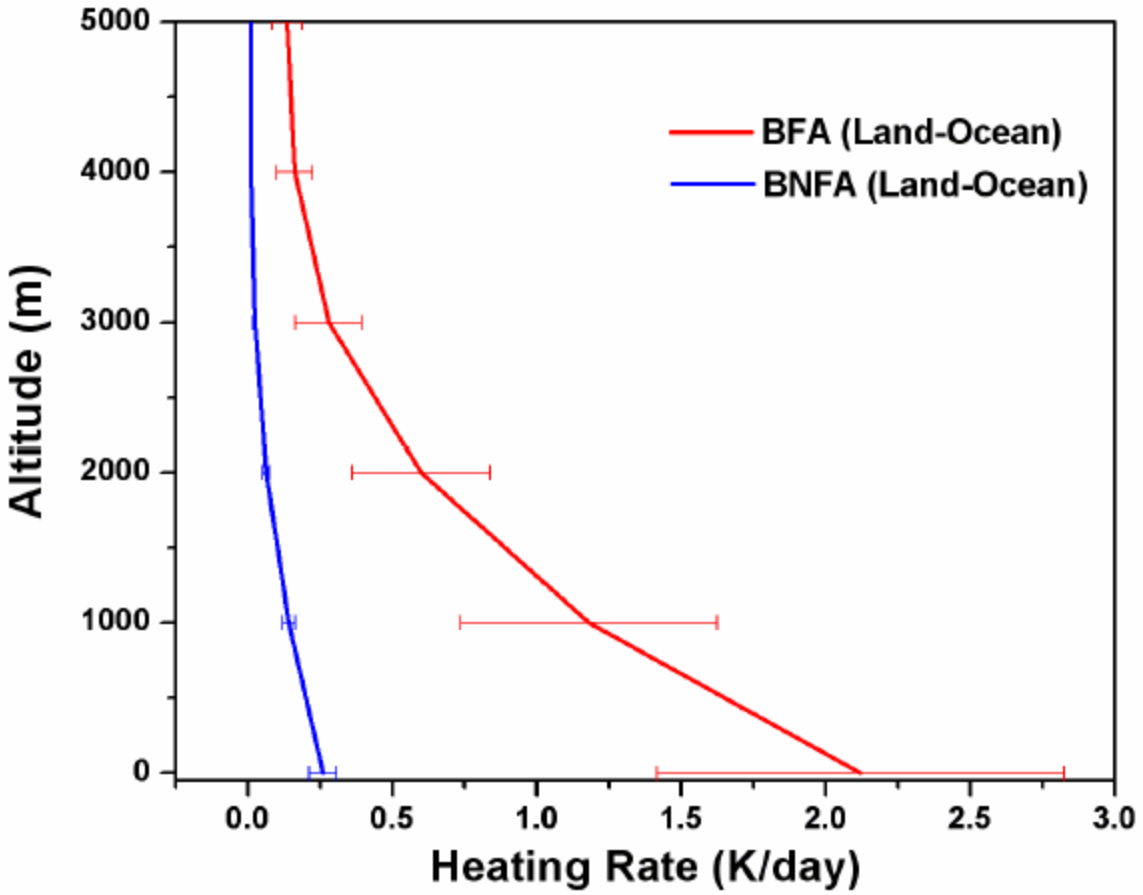

Fig. 10 Vertical profile of difference of aerosol-induced heating rate over Land and Ocean during BFA break and BNFA cases.

Conclusions

- Discovered a fundamental aspect of absorbing aerosol and MISO interaction
- By helping transition of breaks to active conditions Absorbing Aerosols play a crucial role in the MISO transitions
- The fact that those breaks that are associated with strong convection in the NE region, highlight strong interaction between circulation and aerosols
- Dynamic aerosol interaction is required for prediction and simulation of MISO

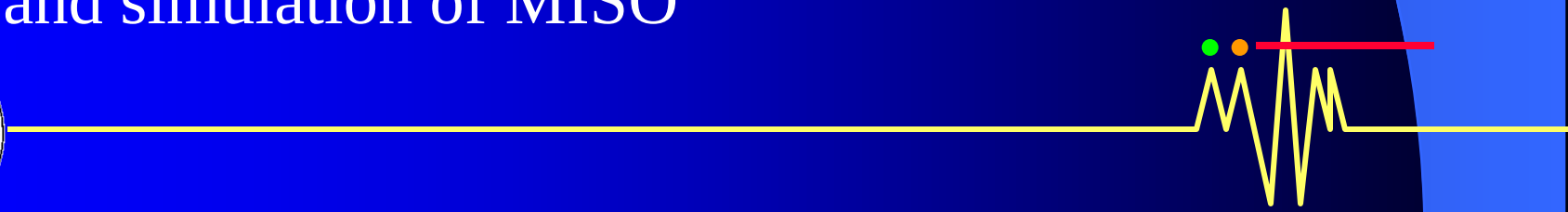

Thank you

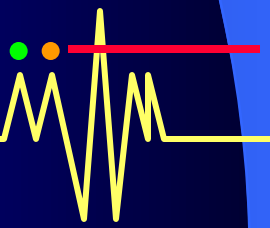

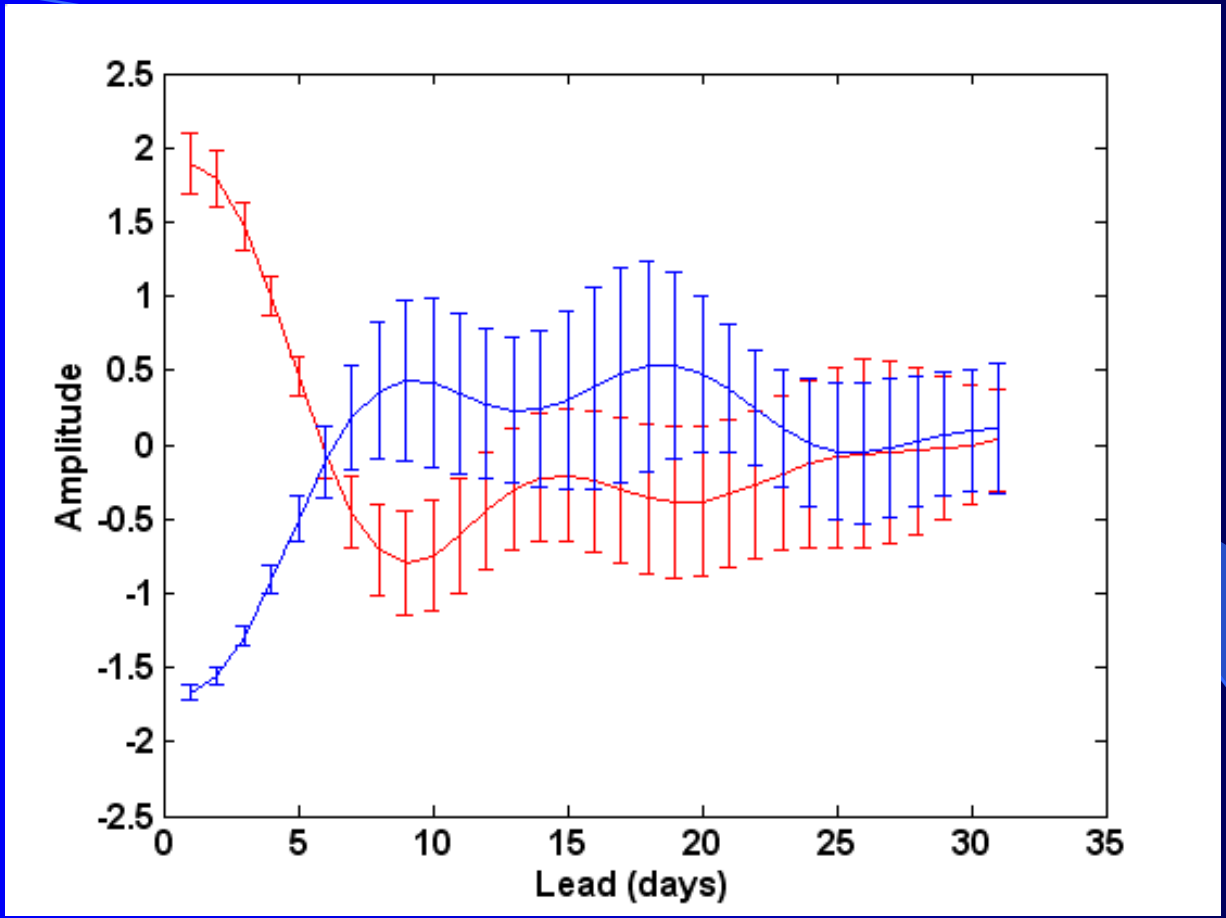

Mean and variance of among different ISO events during a 15 year period corresponding to different lead days starting from peak active (solid) and peak break (dashed) conditions. The curve shows the evolution of mean states and the error bars give variance among different ISO events corresponding to each lead day.

Variability in evolution from active to break and from break to active.

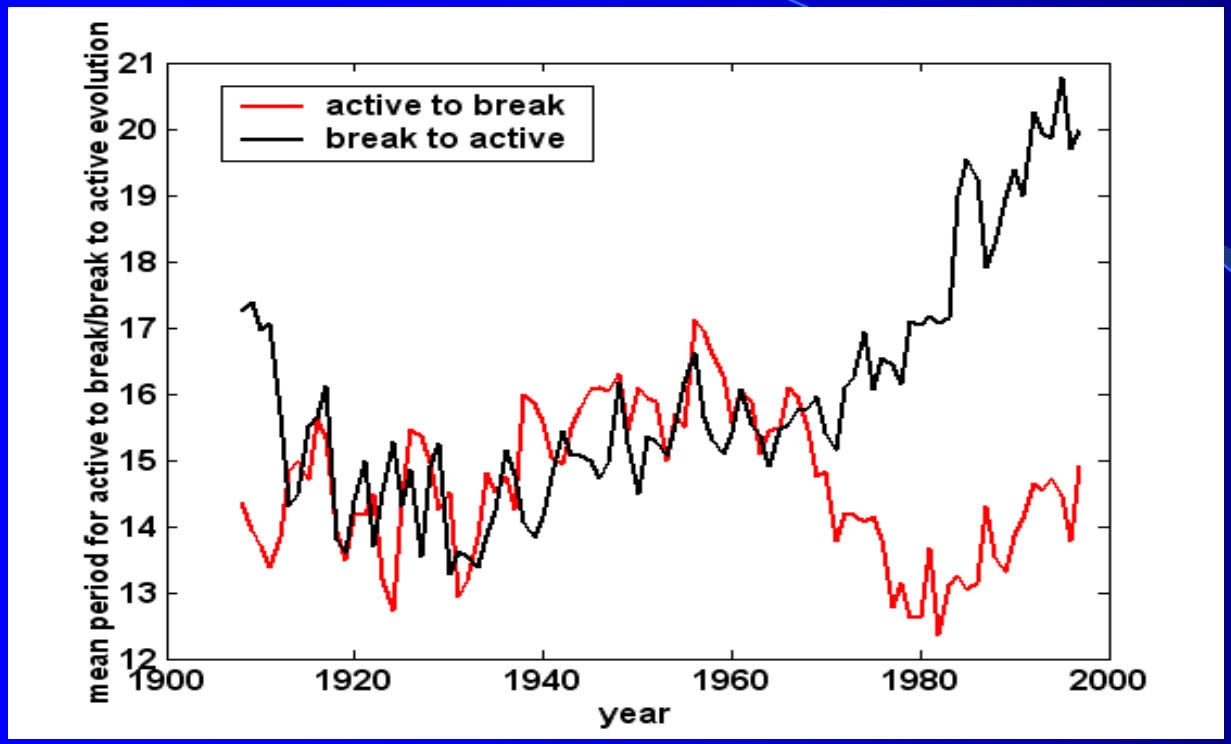

The mode of evolution is another factor determining potential predictability. A slower evolving event is considered to have higher potential predictability than a faster evolving event.

Along with the reduced initial errors, the slower rate of evolution from break to active would also favor an increase in potential predictability of the active phases.